Top Curr Chem (2012) 312: 1–66
DOI: 10.1007/128_2011_218

Published online: 5 October 2011

Charge Transport in Organic Semiconductors

Heinz Bässler and Anna Köhler

Abstract Modern optoelectronic devices, such as light-emitting diodes, field-effect transistors and organic solar cells require well controlled motion of charges for their efficient operation. The understanding of the processes that determine charge transport is therefore of paramount importance for designing materials with improved structure-property relationships. Before discussing different regimes of charge transport in organic semiconductors, we present a brief introduction into the conceptual framework in which we interpret the relevant photophysical processes. That is, we compare a molecular picture of electronic excitations against the Su-Schrieffer-Heeger semiconductor band model. After a brief description of experimental techniques needed to measure charge mobilities, we then elaborate on the parameters controlling charge transport in technologically relevant materials. Thus, we consider the influences of electronic coupling between molecular units, disorder, polaronic effects and space charge. A particular focus is given to the recent progress made in understanding charge transport on short time scales and short length scales. The mechanism for charge injection is briefly addressed towards the end of this chapter.

Keywords Charge carrier mobility · Charge transport · Organic semiconductors · Molecular model · Gaussian disorder model · SSH model · Organic optoelectronics

Contents

H. Bässler (✉) and A. Köhler
Experimental Physics II, University of Bayreuth, Bayreuth, Germany
e-mail: baessler@staff.uni-marburg.de

1 Introduction

Charge transport in organic semiconductors is a timely subject. Today, organic semiconductors are already widely used commercially in xerography. For display and lighting applications they are employed as light emitting diodes (LEDs or OLEDs) or transistors, and they are making progress to enter the solar cell market [1–6]. As a result, interest in the science behind this novel class of materials has risen sharply. The optoelectronic properties of organic semiconductors differ from that of conventional inorganic crystalline semiconductors in many aspects and the knowledge of organic semiconductor physics is imperative to advance further with the associated semiconductor applications [7]. A central problem is the understanding of the mechanisms related to charge transport.

It may seem odd to write an article entitled "charge transport in organic semiconductors," notably polymers, when these materials are inherently insulators. This raises the question about the difference between a semiconductor and an insulator. The conductivity κ of the materials is the product of the elementary charge e, the mobility μ of charge carriers, and their concentration n, i.e., $\kappa = en\mu$. A material can be insulating either if there are no charges available or if they are immobilized. A prototypical example of the former case is quartz. Since the absorption edge of quartz is far in the ultraviolet region (at about 120 nm), the gap E_g between the valence and conduction band is about 10 eV [8]. This implies that, at ambient temperature, the concentration of free charge carriers is practically zero. However, if one generates charge carriers by high energy radiation, they would probably move with a mobility that is comparable to that of a conventional covalently bonded inorganic semiconductor such as silicon, i.e., 1,000 $cm^2\ V^{-1}\ s^{-1}$ or larger. Obviously, an inherent insulator can be converted into a semiconductor if free

charge carriers are generated by either injection from the electrodes, by doping, or by optical excitation.

In traditional semiconductors such as silicon, germanium, or Ga_2As_3 the conductivity is between, say, 10^{-8} to 10^{-2} Ω^{-1} cm^{-1}. In an undoped solid, the concentration of free charge carriers is determined by $n = N_{eff} e^{-\frac{E_g}{2kT}}$ where N_{eff} is the effective density of valence or conduction band states and E_g is the band gap. For crystalline silicon, E_g is 1.1 eV and the charge carrier mobility is about 1,000 cm^2 V^{-1} s^{-1}. This predicts an intrinsic conductivity of about 10^{-6} Ω^{-1} cm^{-1} at room temperature. Note that a band gap of 1.1 eV translates into an absorption edge of 1,100 nm. In view of the relative dielectric constant as large as $\varepsilon = 11$, coulomb effects between electrons and holes are unimportant and electrons and holes are essentially free at room temperature. This implies that optical absorption is due to a transition from the valence band to a conduction band. The situation is fundamentally different in undoped molecular solids. Their absorption edge is usually larger than 2 eV and the dielectric constant is 3–4. In this case optical absorption generates coulomb bound electron-hole pairs with a binding energy of 0.5–1.0 eV. Even if one were to ignore the exciton binding energy and to identify incorrectly the optical absorption edge with a valence to conduction band transition, the resultant intrinsic conductivity would be much less than 10^{-12} Ω^{-1} cm^{-1}, assuming a charge carrier mobility of 1 cm^2 V^{-1} s^{-1}, i.e., the materials are insulators. However, they can become semiconducting if charge carriers are generated extrinsically.

This chapter focuses on the electronic transport of organic semiconductors. The motivation is straightforward. Modern optoelectronic devices, such as light-emitting diodes, field effect transistors, and organic solar cells are based on charge transport. The understanding of the processes that control charge transport is therefore of paramount importance for designing materials with improved structure property relations. Research into this subject was essentially stimulated by studies on charge transport in molecularly doped polymers that are now commonly used in modern photocopying machines. It turns out that xerography is meanwhile a mature technology [1]. It is the only technology in which organic solids are used as active elements on a large industrial scale. An important step in the historic development of xerography was the recognition that one could profitably use aromatic molecules as a photoreceptor when they are embedded in a cheap inert flexible binding material such as polycarbonates. Meanwhile, most photocopiers and laser printers use this kind of receptors although few users will recognize that once they push the print button they start an experiment on transient photoconductivity in a polymeric photoreceptor. There is much hope that organic LEDs, FETs, and solar cells will be able to meet the competition from existing technology based upon inorganic materials and enter the market, similarly to xerography. OLEDs that are based on small molecules already constitute a substantial business.

Apart from the endeavor to optimize the structure property relations of materials used in modern optoelectronic devices there is the desire to understand the conceptual premises of charge transport in random organic solids. The use of amorphous, instead of crystalline, organic semiconductor materials is favored

because they allow for a low cost of device fabrication and the use of flexible substrates, thus enabling mechanically flexible devices. The aim of this chapter is to introduce those new to this field to the already established understanding of charge transport in organic semiconductors, and to point those familiar with the field to current research activities where new insight emerges and to the challenges that remain.

2 Basic Concepts of Charge Transport in Organic Solids

2.1 Electronic Structure of Organic Solids

In order to understand charge transport in organic solids, we need to elaborate on the electronic structure of organic solids. Organic solids such as molecular crystals, amorphous molecular films, or polymeric films are made of molecular subunits. We shall therefore start from a molecular picture and consider any coupling between the molecular units afterwards. Organic semiconductors are hydrocarbon molecules with a backbone of carbon atoms. The strong bonds that form the molecular backbone arise from sp^2 hybridized atomic orbitals of adjacent carbon atoms that overlap yielding a bonding and antibonding molecular σ and σ^* orbitals. The remaining atomic p_z orbitals overlap to a lesser degree, so that the resulting molecular π and π^* orbitals are less binding or antibinding, thus forming the frontier orbitals of the molecule. In the ground state of the molecule, all bonding orbitals up to the highest occupied molecular orbital, the HOMO, are filled with two electrons of antiparallel spin while the antibonding orbitals, from the lowest unoccupied molecular orbital (LUMO) onwards, are empty. Neutral excited states can be formed for example by light absorption in a molecule, when an electron is promoted from the HOMO to the LUMO. In general, any configuration with an additional electron in an antibonding orbital and a missing electron in a bonding orbital, i.e., a hole, corresponds to a neutral excited state. Due to the low relative dielectric constant in organic semiconductors (on the order of $\varepsilon \approx 3$), coulomb attraction between electron and hole is strong, resulting in an exciton binding energy ranging from of 0.5 eV to more than 1 eV. Molecular orbital diagrams corresponding to the configurations in the ground or neutral excited states are shown in Fig. 1.

For charge transport in organic solids to take place, there must be a charge on the molecular unit. This may either be an additional electron that is accommodated in an antibonding orbital, or one that is removed from a bonding orbital. The molecule is then no longer in the ground state but rather in a charged excited state. The addition or removal of an electron from the molecule may be obtained in several ways:

1. Through injection or extraction of an electron at the interface between a metal electrode and the molecule, as is typically the case in the operation of a device such as light-emitting diodes (LED).

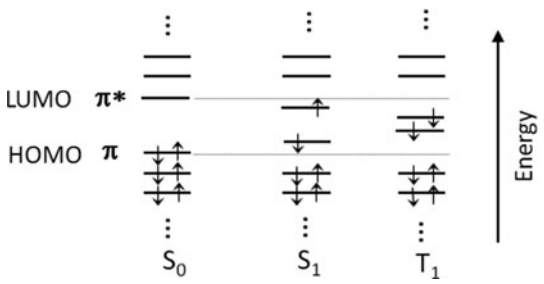

Fig. 1 Molecular orbital diagram showing the electronic configuration for the ground state (S_0), for the first spin-singlet excited state (S_1) and for the first spin-triplet excited state (T_1). The *arrows* indicate the electron spin, the *thin horizontal gray line* is a guide to the eye. In this representation, coulomb and exchange energies are explicitly included in the positions of the frontier orbitals

2. Through reduction or oxidation of the molecule by a dopant molecule. Atoms or molecules with high electron affinity, such as iodine, antimony pentafluoride ($SbCl_5$), or 2,3,5,6-tetrafluoro-7,7,8,8-tetracyanoquinodimethane (F_4-TCNQ), may oxidize a typical organic semiconductor such as poly(*p*-phenylene) derivatives, leaving them positively charged. Reduction, i.e., addition of an electron, may be obtained by doping with alkali metals.
3. Through exothermic dissociation of a neutral excited state in molecule by electron transfer to an adjacent molecule. This process leads to the generation of geminately bound electron-hole pairs as precursors of free positive and negative charges in an organic solar cell.

From electrochemical experiments it is well known that, after the removal of one electron from an individual molecule, more energy is required to remove a second electron. This implies that the relative positions of the molecular orbitals with respect to the vacuum level change upon removal or addition of an electron, as indicated in Fig. 2a in a qualitative fashion. Furthermore, when an electron is taken from a π-orbital or added to a π* orbital, this alters the spatial distribution of electrons in the more strongly bound σ-orbitals, resulting in different bond lengths of the molecule. The energy associated with this change in molecular geometry is known as the geometric reorganization energy, and the charge in combination with the geometric distortion of the molecule is referred to as a polaron. These effects due to electron–electron correlations and electron–phonon couplings are a manifestation of the low dielectric constant of organic semiconductors. They are absent in inorganic semiconductor crystals due to the strong dielectric screening with $\varepsilon \approx 11$.

A charged molecule may absorb light in the same fashion as does a neutral molecule, thereby promoting an electron from a lower to a higher molecular orbital. Possible optical transitions are indicated in Fig. 2a by arrows. These optical transitions can easily be observed in doped molecular films as well as in solution (see below). We note that, analogous to transitions in neutral molecules, absorption

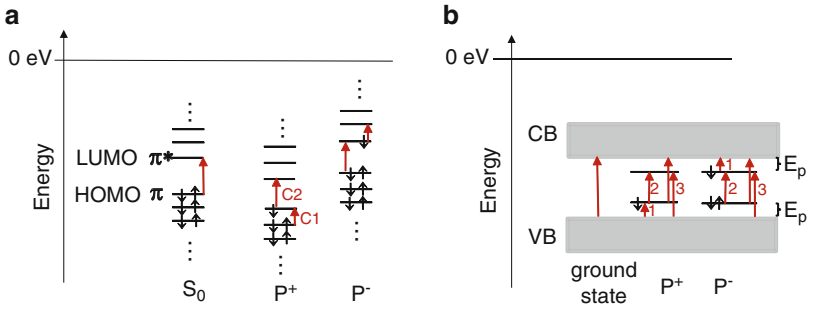

Fig. 2 (**a**) Molecular orbital diagram for a neutral molecule in the ground state (S_0), for a positively charged molecule (P^+), and for a negatively charged molecule (P^-). The shifts in the molecular orbital levels upon charging are only drawn in a qualitative fashion. Optical transitions are indicated by *red arrows*. C1 and C2 label the transitions seen in Fig. 4 further below. (**b**) Semiconductor band picture showing self-localized polaron energy levels within the band gap. The polaron binding energy E_p is also indicated. Predicted optical transitions involving the positive or negative polaron (P^+ or P^-, respectively) are indicated through *red arrows* and labeled by numbers

may cause a transition into different vibrational levels of the charged molecule, thus giving rise to vibrational structure in the polaron absorption spectra.

When molecules are not in a gas phase but in a solid, the absolute values of their energy levels shift with respect to the vacuum level due to the change in the polarization of their surroundings. If they are deposited, by spin-coating or evaporation, to form an amorphous film, the surrounding polarization varies spatially in a random fashion leading to a random distribution of the absolute values of the molecular energies. By the central limit theorem of statistics, this implies a Gaussian distribution of excited state energies [9] for both neutral and charged excited states, with a variance σ that is characteristic for the energetic disorder. Experimentally, this is observed as an inhomogeneous broadening of the optical spectra such as absorption, fluorescence, and phosphorescence spectra. Hole and electron transporting states are similarly disorder broadened although in this case state broadening is not directly amenable to direct absorption spectroscopy.

Such disorder is absent in a molecular crystal. In an inorganic semiconductor crystal, such as Si or Ge, atoms are bound by strong covalent bonds to form the crystal. Consequently, electronic interactions between the atomic orbitals are strong, and wide bands with bandwidths on the order of a few eV are formed that allow for charge transfer at high mobilities. In contrast, molecular crystals are kept together by weak van der Waals bonds. Consequently, electronic interactions between the molecular orbitals of adjacent lattice sites are weak and the resulting bands are narrow, with bandwidth below 500 meV [10]. In very pure molecular crystals of, say, naphthalene or perylene, band transport can therefore be observed from low temperatures up to room temperature [11–14]. At higher temperatures, intra- and intermolecular vibrations destroy the coherence between adjacent sites. A charge carrier is then scattered with a mean free path that approaches the distance

between adjacent sites. As a result, band transport is no longer possible and charge carriers move by hopping.

On passing, we note that even though charge transport in pure molecular crystals takes place in a band, optical transitions in a molecular crystal do NOT take place between valence and conduction bands due to a lack of oscillator strength. This is an inherent consequence of the strong coulomb interaction present between charges in molecular crystals. While in inorganic crystals, the strong dielectric constant implies an effective shielding of coulomb forces, this is not the case in organic crystals due to their low dielectric constant. It implies that when an optical transition is to take place, in order for an electron to escape from its coulombically bound sibling, it had to overcome a coulomb capture radius which is about 20 nm. The electronic coupling among molecules that far apart is negligibly small, resulting in a negligible oscillator strength for such a "long distance charge-transfer type" transition. Therefore, a transition such that the electron is outside the coulomb capture radius of its sibling does not take place. Rather, absorption and emission in a crystal takes place between orbitals of an individual molecule on a particular lattice site, or between orbitals of immediately adjacent molecules, thus yielding strongly coulombically bound electron hole pairs, referred to as Frenkel excitons or charge transfer excitons, respectively. In a perfectly ordered crystal, the exciton, i.e., the two-particle excitation, is equally likely to be on any lattice site and thus couples electronically to neighboring sites. This results in the formation of an exciton band, i.e., a band for the two-particle excitation, within which the exciton moves in a delocalized fashion. Note that the exciton band describes the electronic coupling between an existing two-particle excitation on a molecule with its neighboring site (and thus the motion of an exciton), while the π or π^* bands describe the coupling of a one-particle molecular orbital with its neighbor. π or π^* bands are therefore suitable to portray the motion of a single charge carrier in a molecular crystal, yet, for the reasons just outlined, optical transitions between them do not occur.

Today's organic semiconductor devices such as LEDs, FETs, or solar cells may be made from amorphous molecular films, molecular crystals (in the case of some FETs), or from polymeric semiconductors. In polymers, molecular repeat units are coupled by covalent bonds allowing for electronic interaction between adjacent repeat units. As will be detailed in the next section, in a perfectly ordered polymer, such as crystalline polydiacetylene [15], this electronic interaction leads to the formation of a broad intra-chain exciton band as well as valence and conduction bands while inter-chain interactions are moderately weak and comparable with the situation of molecular crystals. In amorphous polymers, conformational disorder implies that coherence is only maintained over a few repeat units that thus form a chromophore [16]. We refer to this section of the polymer chain as the conjugation length. Naturally, the conjugation length in rigid, well ordered polymers such as MeLPPP is longer (on the range of 10–15 repeat units) than in polymers with a high degree of torsional disorder along the chain such as DOO-PPP [17, 18]. A charge carrier on a polymer chain may move coherently within the conjugation length, though hopping will take place between different conjugated segments [19, 20]. For the purpose of considering charge transport, it is therefore convenient to treat

a conjugated segment of a polymer chain as a chromophore, i.e., analogous to a molecule.

So far we have outlined the conceptual framework in which we discuss charge transfer in organic semiconductors. It is based on a molecular picture where the molecular unit is considered central, with interactions between molecular units added afterwards. For amorphous molecular solids and for molecular crystals this approach is undisputed. In the case of semiconducting polymers, a conceptually different view has been proposed that starts from a one-dimensional (1D) semiconductor band picture, and that is generally known as the Su–Schrieffer–Heeger (SSH) model [21–24].

We feel the molecular approach we have taken gives an appropriate description of the underlying electronic structure. The conceptual framework one adopts however influences the interpretation of experimental results, for example when considering the absorption spectra of charge carriers. In order to place the discussion of charge transfer models for polymers into a larger context, it is beneficial to be aware of agreements and differences between a "molecular approach" and the SSH model. Therefore we shall digress here to a comparative discussion of the two approaches.

2.2 *Comparison of the Molecular Picture and the SSH Approach of Treating Charge Carriers in Semiconducting Conjugated Polymers*

The theory for a band picture of semiconducting polymers has been developed for a perfect, infinite, one-dimensional polymer chain. The simplest case to consider is polyacetylene, i.e., a chain of sp^2-hybridized carbon atoms. Early work on this "system" was carried out in the 1950s by Salem and Longuett-Higgins [25], who considered the electronic structure of a long sp^2-hybridized carbon chain with cyclic boundary conditions, i.e., forming a ring. The effect of a charge on such a system was later investigated by Su, Schrieffer, and Heeger [21], after synthesizing and doping polyacetylene. A similar theoretical "system" to consider is an infinite, planar chain of poly(*p*-phenylene) (PPP), which can be considered analogous to a one-dimensional "crystal" of phenyl units with strong coupling between the units. From an experimental point of view, a good realization of a perfect one-dimensional semiconducting polymer chain is given by crystalline polydiacetylene [15].

We will first sketch briefly how the electronic structure of a perfect one-dimensional polymer chain is perceived in a molecular picture before drawing the comparison to a semiconductor band picture. For our molecular based approach, we consider, say, a perfect PPP chain as a sequence of molecular repeat units such as phenylenes that are coupled by a covalent bond. As a result of the coupling, the molecular orbitals of adjacent units can interact and split. Due to the perfect order and symmetry, this process takes place across the entire chain leading to the

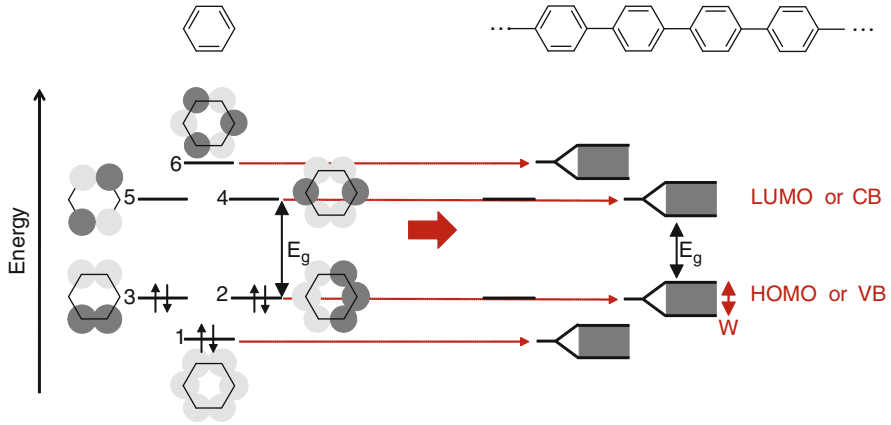

Fig. 3 Schematic, qualitatively illustrating the formation of bands from molecular orbitals when going from benzene to a perfectly ordered, infinite poly(*p*-phenylene) (PPP). (**a**) Energies and shapes of molecular orbitals for benzene in a simple Hückel-type picture. (**b**) Qualitative band structure resulting from electronic coupling between orbitals with electron density at the para-position. The frontier orbitals 2 and 4 in benzene can delocalize along the entire PPP chain, thus forming valence and conduction bands of width W. The lower and higher lying orbitals 1 and 6 in benzene can form corresponding lower and higher lying bands. Orbitals with nodes at the para-position such as 3 and 5 remain localized. See also [26]

formation of bands. For example, π and π* bands will arise from HOMO and LUMO orbitals, and they will take the role of a valence and conduction band. This is schematically illustrated in Fig. 3. In the molecular picture, coulomb interactions are considered to be strong, and consequently, for the same reasons as outlined in the case of a three-dimensional molecular crystal, optical excitations in a perfect polymer chain are assumed to result in the formation of strongly bound electron-hole pairs while direct transitions from a valence π-band to a conduction π* band are expected not to carry any oscillator strength. The π and π* bands in a perfect polymer in a perfect crystalline environment, and the energy gap separating them, owe their existence to the electronic coupling between repeat units. Their existence is independent of whether the system is aromatic or whether it has an alternation of single/double bonds. A critical quantity, however, is the relative size of the coupling energy between repeat units compared to the energetic variation of each unit (see Sect. 2.3 below). In amorphous polymer films, energetic disorder due to the polarization of the surroundings is strong, so that electronic coherence is only maintained over a few repeat units that are usually referred to as a conjugated segment.

In contrast, in the SSH model, the electrical bandgap E_g^{el} arises because of the alternation between single and double carbon–carbon bonds, a signature of the Peierls distortion in a 1D system. When a perfect 1D chain of equidistant carbon atoms is considered, the electronic structure resulting from the electronic coupling between the atomic p_z-orbitals is that of a half-filled π band, implying a metallic

character. The introduction of an alternating bond length, however, leads to the formation of a filled π-band and an empty π* band, with a gap separating them, thus predicting semiconducting properties.

One of the key assumptions of the SSH model is that the electron–electron correlations and the coulomb attraction between electrons and holes are very small. As a direct consequence, the optical absorption is assigned to a valence band (VB) to conduction band (CB) transition as is in a conventional semiconductor rather than to the transition into a neutral excitonic state. The second key assumption in the SSH model relates to the magnitude of the electron–phonon coupling. Once a free electron–hole pair has been excited by an optically driven VB–CB transition, electrons and holes couple to phonons regardless if the associated chain distortions are conventional long wavelength phonons or rather more localized molecular vibrations. This type of coupling is inherent to both the molecular model and the semiconductor, i.e., SSH–model. It is a signature of the geometric reorganization a chain suffers when an electron is transferred from the HOMO to the LUMO. The reorganization energy is referred to as the polaron binding energy. The essential difference between the molecular and the SSH model relates to (1) the magnitude of the coupling and (2) the assignment of the sub-bandgap absorption features that show up when electrons and holes are excited. In the SSH model and the related Fesser – Bishop – Campbell model [23] a positively (negatively) charged self localized polaron P^+ (P^-) is created by removal (addition) of an electron with respect to the mid-gap Fermi-energy. As a result two energy levels form inside the band gap that are occupied with a total of one electron (three electrons). The polaron is associated with transitions among localized levels and non-localized band states (see Fig. 2). For example for P^+, the lowest transition is from the VB to a localized level (1), the second next lowest transition is between the localized levels (2), followed by two degenerate transitions (3). This implies that the lowest transition is a direct measure of the polaron binding energy E_p while the second next transition should occur at an energy of $E_g - 2E_p$, taking into account that the optical absorption edge is identified as a VB → CB transition. As a consequence of the neglect of the coulomb binding energy on the one hand and the assumed large electron–phonon coupling on the other, the collapse of two charges of the same kind should be an exothermic process leading to the formation of positively or negatively charged bipolarons. They are predicted to give rise to two sub-band optical absorption features.

Meanwhile there is overwhelming evidence that the basic assumptions of the SSH model are not applicable to π-bonded conjugated polymers. Coulombic and electron–electron correlation effects are large while electron–phonon coupling is moderately weak. As a consequence, the spectroscopic features in this class of materials are characteristic of molecular rather than of inorganic crystalline semiconductor systems. There are a number of key experimental and theoretical results that support this assignment:

1. A material that can be considered as a prototypical one-dimensional system consists of a poly-diacetylene (PDA) chain embedded in a perfect molecular precursor crystal at a concentration low enough that there is no inter-chain interaction. Such systems can be fabricated by controlled irradiation of a precursor crystal [15]. Some of the PDAs fluoresce. The absorption and fluorescence spectra are excitonic in character with resonant 0–0 transitions [15]. The Huang Rhys factor is small, indicating that coupling to molecular vibrations (and phonons) is weak. In conventional absorption spectroscopy the VB → CB transition is absent, although it shows up in electroabsorption spectroscopy. The energy difference of 0.55 eV between the exciton transition and the valence π-band → conduction π* band transition is a direct measure of the exciton binding energy [27]. This value is supported by theory. In other π-conjugated polymers the magnitude of the exciton binding energy is similar [28]. In passing, we note that if the exciton binding energy was only about kT as implied by the SSH model there should be no efficient electroluminescence in organic LEDs, since in the absence of coulomb attraction electrons and holes would hardly find each other [29].
2. Level crossing between the two lowest singlet excited states was observed by the Kohler group through absorption and luminescence spectroscopy in oligoenes when the oligomer chain length increases. This can only be accounted for when electron–electron correlations are strong [30]. Another signature of the strong electron–electron interactions in π-bonded conjugated polymers is the observation of phosphorescence [31–34]. Phosphorescence spectra are separated from the fluorescence spectra by an exchange interaction energy of about $2J = 0.7$ eV (where J is the value of the exchange integral) [34, 35], implying a strong electron correlation effect.
3. The fact that the lowest charge induced absorption feature in π-conjugated polymers is near 0.5 eV is in disagreement with the notion that it is due to a transition involving a localized state and a band state, thus reflecting the magnitude of the polaron binding energy, which is half of the total reorganization energy $E_p = \frac{\lambda}{2}$. Even if one interpreted the temperature dependence of the hole mobility in the ladder type poly(*p*-phenylene) LPPP in terms of a disorder-free polaron transport (thus attributing all activation energy to polaronic effects) one would end up with a value of the polaron binding energy as low as 50 meV [36].
4. There is convincing evidence that the absorption spectra of charged π-conjugated oligomers and polymers are electronic transitions among different electronic levels of (monovalent) radical anions and cations rather than bipolarons (see, for example, Fig. 4) [37]. The spectra do not reflect the reorganization energy involved in ion formation but bear out vibronic splitting and follow the same relation on the reciprocal chain length dependence as do the absorption spectra of uncharged oligomers. However, in the experiments reported in [37] it has been observed that upon increasing the concentration of the oxidant/reductant the absorption features are shifted to higher energies. One could surmise that at high ion concentration bipolarons are indeed formed. Meanwhile it has been

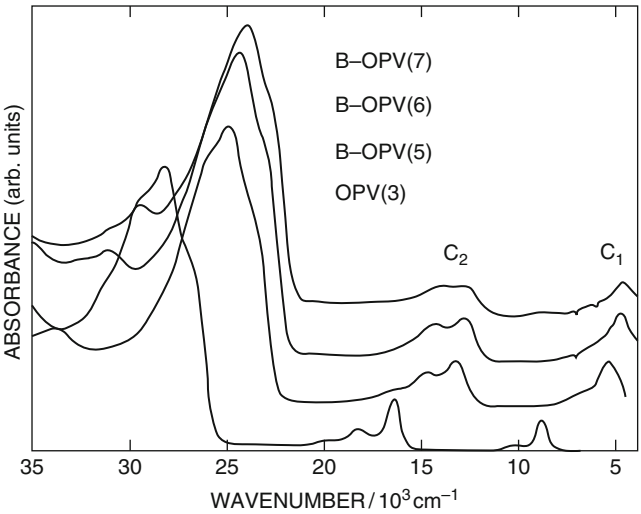

Fig. 4 Absorption spectra of radical cations of oligo-phenylenevinylenes OPV of different chain lengths in CH_2Cl_2 solution. C_1 and C_2 denote the transitions indicated in Fig. 2a. The radical ions are generated by adding $SbCl_5$ as an oxidant to the solution. From [37] with permission. Copyright (1993) by Elsevier

suggested, though, that the high energy features are due to the formation of pairs of monovalent polarons in which the radical ion state splits into a doublet in which the lower state is doubly occupied [38]. Related work has been performed on polyazulenes [39, 40]. Nöll et al. find that polyazulene can be doped up to a maximum number of one positive charge per three to four azulene units. At these high doping levels the charge carrying units are pairs of single-valent radical cations rather than bipolarons. At still higher doping levels the polymer starts decomposing. The energetic instability of bipolarons has further been proven by quantum chemical calculations on model systems consisting of a ring of thiophene units. The result is that, upon adding a second charge to the ring, both charges avoid each other rather than form a stable bipolaron [41]. More recent work indicates that a stable entity may only be formed when a pair of like charges is coupled with an oppositely charged moiety (a "trion") in which the coulomb repulsion is diminished [42]. Obviously the coulomb repulsion between a pair of like charges exceeds the gain in reorganization energy. Therefore bipolarons are unstable [43, 44]. By the way, it has never been questioned that the charge carrying species that is monitored in charge transport studies is a singly rather than a doubly charged entity.

This digression on the interpretation of the absorption from charged polymers illustrates the importance of the conceptual framework that is adopted. As already mentioned, for molecular glasses or crystals, a molecular picture has always been undisputed. For polymers, the debate conducted over the last two decades has

eventually been largely settled on the same molecular view. Consequently, the discussion of the charge transfer models in this chapter is also based on a molecular picture throughout.

2.3 General Approach to Charge Transfer Mechanisms

There is quite a range of charge transfer models based on the molecular picture that are employed to describe charge transport in organic solids, such as models based on band transport, polaronic models, and models that focus on the effects of disorder. At the same time, organic solids are a broad class of materials, comprising crystals as well as molecular and polymeric glasses. It is therefore necessary to obtain some basic understanding on which parameters affect charge transport in order to assess which model may be suitable to describe a particular experimental situation.

In order to develop such a broader view and a general qualitative understanding of charge transport, it is beneficial to consider the general one-electron Hamiltonian shown in (1). In this approach we follow the outline taken in [45]. This Hamiltonian assumes a low carrier density, and effects due to electron correlation or coulomb interaction are not considered. Despite these limitations, the following general one-electron Hamiltonian is useful to illustrate different limiting cases:

$$H = H_0 + H_1 + H_2 + H_3 + H_4 \tag{1}$$

with

$$H_0 = \sum\nolimits_n \epsilon_n a_n^\dagger a_n + \sum\nolimits_\lambda \hbar\omega_\lambda \left(b_\lambda^\dagger b_\lambda + \frac{1}{2} \right)$$

being the electronic and vibrational excitation term,

$$H_1 = \sum\nolimits_{\substack{n,m \\ n \neq m}} J_{nm} a_n^\dagger a_m$$

being the electron transfer term,

$$H_2 = \sum\nolimits_\lambda \sum\nolimits_n g_{n\lambda}^2 \hbar\omega_\lambda a_n^\dagger a_n \left(b_\lambda + b_{-\lambda}^+ \right)$$

being the dynamic diagonal disorder term,

$$H_3 = \sum\nolimits_{\substack{n,m \\ n \neq m}} \sum\nolimits_\lambda f_{nm\lambda}^2 \hbar\omega_\lambda a_n^\dagger a_m \left(b_\lambda + b_{-\lambda}^\dagger \right)$$

being the dynamic off-diagonal disorder term, and

$$H_4 = \sum\nolimits_n \delta\epsilon_n a_n^\dagger a_n + \sum\nolimits_{\substack{n,m \\ n\neq m}} \delta J_{nm} a_n^\dagger a_m$$

being the static diagonal and off-diagonal disorder term.
$a_n^\dagger$ (a_n) is the creation (destruction) operator for an excited electron in an orbital of energy ε_n at the molecular site n,
$b_n^\dagger$ (b_n) is the creation (destruction) operator for an vibrational mode of energy $\hbar\omega_\lambda$,
ε_n is the energy in a perfectly ordered lattice and $\delta\varepsilon_n$ is its variation due to static disorder,
J_{nm} is the electronic interaction between site m and n in a perfectly ordered lattice and δJ_{nm} is its variation due to static disorder, and
$g_{n\lambda}$ and $f_{nm\lambda}$ are dimensionless coupling constants for the electron–phonon coupling.

In (1), H_0 yields the total energy of system in which the molecules and the lattice are excited, yet there are no interactions between molecules and the lattice. The transfer of an electron from site m to site n is given by H_1. Polaronic effects, i.e., effects due to the interaction of the electronic excitation and the lattice, are given by H_2 and H_3. In H_2, the energy of the site is reduced by the interaction with the lattice vibration. In H_3, the lattice vibration alters the transition probability amplitude from site m to n. The term lattice vibration may refer to inter-molecular or intra-molecular vibrations. Static disorder effects are considered in H_4, which describes the changes to the site energy or transition probability amplitude by variations in the structure of the molecular solid.

The interactions considered in the polaronic terms H_2 and H_3 introduce "dynamic" disorder, since they are based on coupling of the electronic excitation to lattice vibrations. In contrast, the changes to site energy and transition rate in H_4 are independent of vibrations. They are merely due to variations in the morphological structure of the film or crystal, i.e., intermolecular distances and orientations, and they are thus referred to as "static" disorder. When (1) is written out in a matrix notation, the site energies appear on the diagonal position of the matrix, and thus energetic variations are sometimes called "diagonal disorder" while changes in the transition rate from site n to m are disguised by the term "off-diagonal disorder." In the Hamiltonian of (1), only linear coupling to lattice vibrations is considered. Throughout this chapter, the expression "disorder" usually refers to static disorder only, while we tend to employ the expression "polaronic effects" to discuss the effects due to the electron–phonon coupling expressed in H_2 and H_3.

Having clarified some of the terminology used, we can now turn to considering different modes of charge transfer. The nature of charge transfer is determined by the relative sizes of the interaction energy J_{nm}, the strength of the electron–phonon coupling expressed though the coupling constants in $g_{n\lambda}^2\hbar\omega_\lambda$ and $f_{nm\lambda}^2\hbar\omega_\lambda$, and the degree of static disorder present and expressed through $\delta\varepsilon$ and δJ_{nm}. Essentially, there are three limiting cases.

2.3.1 Band Transport

If the interaction energy with nearest neighbor, $J_{n,n+1}$,is large compared to any other energy present such as the effects of dynamic or static disorder, charge transport takes place through a band. The charge carrier delocalizes to form a propagating Bloch wave that may be scattered by lattice vibrations. Band transport can only occur if the bands are wider than the energetic uncertainty of the charge carrier. This requirement implies that by zero order reasoning [45] the charge carrier mobility must very roughly exceed $ea^2W/\hbar kT$, where e is the elementary charge, a is the lattice constant, and W is the bandwidth. For organic semiconductors, $W \approx 10\ kT$ and $a \approx 1$ nm so that band transport occurs if $\mu \approx 10\ \mathrm{cm}^2\ \mathrm{V}^{-1}\ \mathrm{s}^{-1}$.

2.3.2 Polaronic Transport

If H_1 is small compared to H_2 and H_3, and if H_4 can be neglected, the transport is dominated by the coupling of the electronic excitation to intermolecular or intramolecular vibrations, and the charge carrier coupled to the lattice is termed a polaron. The interaction expressed in term H_2 causes a reduction of the site energy by the polaron binding energy. For charge transport, this needs to be overcome by thermal activation. The charge transfer itself takes place by an uncorrelated, phonon-assisted hopping process, and it is determined by H_3.

2.3.3 Disorder-Based Transport

If fluctuations in the intermolecular distances and orientations give rise to a large variation in the site energy and transition probability amplitude compared to the other terms, the static disorder dominates the charge transport. A charge carrier moves by uncorrelated hops in a broad density of states. Thermal activation is required to overcome the energy differences between different sites.

These different modes of transport result in a dissimilar temperature dependence of the charge carrier mobility, and this often provides a convenient means to investigate which transport regime may apply. In this chapter, due attention is therefore given to experimental approaches that allow for an investigation of the transport mechanism, and concomitantly of the underlying electronic structure.

In this chapter we start by considering charge transport for materials where the disorder aspect is dominant. This conceptual framework is then extended to include polaronic aspects. After discussing the effects of charge carrier density on charge transport in this disorder + polaronic dominated transport regime, we next consider how a stronger coupling between molecular units alters the mode of charge transport, finally arriving at the regime of band transport. Charge injection, which often precedes charge transport, is briefly addressed at the end of this chapter.

In the context of this chapter, we focus on the undoped or lightly doped π-conjugated systems that are commonly referred to as organic semiconductors. Conducting polymers, such as PEDOT:PSS, plexcore, polyaniline, polypyrrole, and others are not addressed here as their charge transfer mechanisms are rather different and would warrant an article in its own right.

3 Charge Transport at Low Carrier Density

The mobility of charge carrier is a key parameter for the understanding of electronic phenomena in organic semiconductors used, for instance, in electrophotography, and in modern devices such as organic light emitting diodes (OLEDs), field effect transistors (FETs), and photovoltaic (PV) cells. It determines both the device current and, concomitantly, the device efficiency as well as its response time. Devices of practical use are often layers of molecularly doped polymers, vapor deposited π-bonded oligomeric molecules, or π-conjugated main chain polymers. In such systems, disorder is a major issue for the structure–property relation. Since there is already a wealth of understanding of salient disorder phenomena pertinent to charge transport in such systems (see [46]), we shall only summarize earlier achievements and concentrate in more detail on more recent developments instead.

3.1 Experimental Approaches

The classic experiment to measure the mobility μ of charge carriers in a semiconductor is based upon the time of flight (ToF) technique. One creates a spatially narrow sheet of charge carriers next to the semitransparent top electrode in a sandwich-type sample by a short laser pulse and one records its arrival time (transit time) $t_{tr} = \mu/dF$ at the exit contact, d being the sample thickness and F being the electric field. Typically, one observes an initial spike followed by a plateau that falls off with a more or less pronounced kink. The initial spike reflects charge motion prior to the energetic relaxation in the DOS provided that the RC time constant of the device is short. Charges generated high in the density of states have a high hopping rate to neighboring sites since virtually all neighboring sites are at lower energy, and jumps down in energy are fast. This high hopping rate translates in a high current. Once in thermal equilibrium, the hopping rate is slower, reflected in a moderate and constant current. The initial spike is thus a genuine feature of a ToF signal in an amorphous film unless charge carriers are generated site-selectively at tail states of the DOS [47]. Experiments on molecularly doped polymers bear out this phenomenon consistently. It is not present in molecular crystals, where the mobility is time-independent. While the position of the kink in the current vs. time plot gives the transit time, the sharpness of the kink at the end of the plateau, i.e.,

the broadening of the signal, is a measure of the diffusion of the charge carriers while they are drifting under action of the applied field F. However, to observe ideal ToF signals requires that (1) the sample is free of charges without photoexcitation implying that the dielectric relaxation time $\varepsilon\varepsilon_0/\kappa$ is large compared to the transit time t_{tr}, (2) the RC-time constant is small compared to the transit time t_{tr}, (3) the thickness of the spatial spread of the packet of charge carriers is small compared to the film thickness d, (4) the concentration of charges is low enough that the charges do not interact, (5) there is no deep trapping, and (6) the mobility is time independent. Under intrinsic optical charge generation, condition (3) requires that the sample thickness is much larger than the penetration depth of light which is at least 100 nm or even larger. This implies a sample thickness of several micrometers. The problem can be circumvented if charges are photoinjected from a thin sensitizing dye layer [48]. This method has been applied to samples as thin as 300 nm [49]. Regarding condition (4), one usually assumes that it is fulfilled if the number of transported charges is less that 5% of the capacitor charge in order to prevent distortion of the ToF signal. For a field of 10^5 V/cm, a dielectric constant ε of 3 and a film thickness of $d = 2$ μm implies that the concentration of mobile charges inside the samples is smaller than 10^{15} cm^{-3} while a film thickness of 100 nm leads to a concentration of about 2×10^{16} cm^{-3}. These numbers suggest about 10^{-6} or, respectively, 2×10^{-5} charges per transport unit. The latter can be a molecule or a segment of a conjugated polymer. In order to overcome the problem of the RC time constant of the device exceeding the charge carrier transit time in thin samples, Klenkler et al. applied a transient electroluminescent technique to measure the electron mobility in Alq_3 [50]. The technique is fundamentally optical insofar that it decouples the carrier transit signal from the device charging signal, and it is free of RC time constant constraints. However, since it requires the fabrication of multilayer devices, it is applicable to polymer systems only if interlayer penetration can be avoided [51].

An alternative technique to measure the charge carrier mobility involves the injection of a space-charge-limited current from an ohmic electrode. In the absence of deep trapping the current is given by Child's law, i.e., $\varepsilon\varepsilon_0\mu F^2/d$. More recently, Juska et al. developed the technique of extracting charge carrier by linearly increasing voltage (CELIV) to measure μ [52]. In this technique one probes charge transport under steady state conditions. Therefore dispersion effects that are often important in ToF experiments are eliminated. However, the correct evaluation of the CELIV transients produced by photoexcitation nevertheless needs to be carried out with due care [53]. Dispersion effects are also eliminated when monitoring charge flow between coplanar source and drain electrodes in a field effect transistor. In an FET a variable gate voltage modulates a current injected from one of the electrodes. Since the number of charges is determined by the sample capacitance, the current is a direct measure of the carrier mobility. It turns out the mobility inferred from an FET-characteristic can exceed the value determined by a ToF experiment significantly. The reason is that the space charge existing in an FET fills up deep trapping states (see Sect. 4.1).

3.2 Conceptual Frameworks: Disorder-Based Models

A basic concept to analyze the charge carrier mobility in a disordered organic solid is the Gaussian disorder model (GDM) [46, 54] that describes hopping in a manifold of sites. In its original version the system is considered as an array of structureless point-like hopping sites with cubic symmetry whose energies feature a Gaussian-type density of energetically uncorrelated states distribution (DOS) with variance σ. The simplest ansatz for the hopping rate is that of Miller and Abrahams [55],

$$\nu_{ij} = \nu_0 \exp\left(-2\gamma a \frac{r_{ij}}{a}\right) \times \exp\left(-\left(\frac{\varepsilon_j - \varepsilon_i}{kT}\right)\right) \qquad \text{for } \varepsilon_j > \varepsilon_i, \tag{2a}$$

$$\nu_{ij} = \nu_0 \exp\left(-2\gamma a \frac{r_{ij}}{a}\right) \times 1 \qquad \text{for } \varepsilon_j \leq \varepsilon_i, \tag{2b}$$

where r_{ij}/a is the relative jump distance between sites i and j, a is the lattice constant, γ is the inverse localization radius related to the electronic coupling matrix element between adjacent sites, and ν_0 is a frequency factor. In a conventional ToF experiment or in Monte Carlo simulations one generates independent charge carriers at energetically arbitrary sites and one follows their motion under the action of an applied electric field. This implies that the charges execute a random walk. In its course they tend to relax energetically towards quasi equilibrium. Asymptotically, an occupational density of states distribution (ODOS) with the same variance yet displaced from the center of the original DOS by σ^2/kT is approached. Subsequent charge transport occurs by thermally activated jumps from the ODOS to a so-called transport energy somewhat below the center of the DOS [56]. This process is terminated when the charges arrive at the exit electrode. During the relaxation process the mean hopping rate, and thus the velocity of the packet of charges, decrease. This implies that the mobility decreases with time until a steady state condition is approached. Depending on the experimental parameters this relaxation process may not be completed before the charge carriers arrive at the exit contact. In a ToF experiment this results in a dispersive signal. In this case the ToF signal shows a featureless decay if plotted in a linear current vs time diagram. Only when displayed using logarithmic scales does a kink mark the arrival of the fastest carriers. However, the inferred "mobility" is no longer a material parameter. Rather it depends on experimental parameters such as sample thickness and electric field. However, even if the energetic relaxation of the charge carriers is completed before they reach the exit contact, the tail of the ToF signal is broader than expected for a hopping system devoid of disorder. The reason is that disorder gives rise to an anomalous spatial spreading of the packet of charges that increases with electric field and degree of disorder [57–61]. It turns out that this spread of the tail, defined as $w = \frac{(t_{1/2} - t_{tr})}{t_{1/2}}$, where $t_{1/2}$ is the time at which the current has decayed to half of

the plateau value, is more or less universal, yielding $w = 0.4$–0.5 for a system in which σ is about 0.1 eV [62].

In an extended version of the hopping concept, positional ("off-diagonal") disorder in addition to energetic ("diagonal") disorder has been introduced [54, 63]. The simplest ansatz was to incorporate this by allowing the electronic overlap parameter $2\gamma a$ to vary statistically. Operationally, one splits this parameter into two site contributions, each taken from a Gaussian probability density, and defines a positional disorder parameter Σ, in addition to the energetic disorder parameter σ.

Monte Carlo simulations [54], analytical effective medium theory [64], and stochastic hopping theory [46] predict a dependence of the charge carrier mobility as a function of temperature and electric field given in (3):

$$\mu(\hat{\sigma}, F) = \mu_0 \exp\left(-\frac{4\hat{\sigma}^2}{9}\right) \exp\left\{C(\hat{\sigma}^2 - \Sigma^2)\sqrt{F}\right\} \quad \text{for } \Sigma \geq 1.5, \tag{3a}$$

$$\mu(\hat{\sigma}, F) = \mu_0 \exp\left(-\frac{4\hat{\sigma}^2}{9}\right) \exp\left\{C(\hat{\sigma}^2 - 2.25)\sqrt{F}\right\} \quad \text{for } \Sigma \leq 1.5, \tag{3b}$$

where $\hat{\sigma} = \sigma/kT$ and C is a numerical constant that depends on the site separation. If the lattice constant $a = 0.6$ nm, then C is 2.9×10^{-4} cmV$^{1/2}$. Equation (3) predicts a Poole Frenkel-like field dependence. It is important to note, though, that the Poole Frenkel-like field dependence is experimentally obeyed within a significantly larger field range than predicted by simple simulation. The reason is that the energies of the hopping sites are essentially determined by the van der Waals interaction between a charged site and its polarizable neighbor sites which may carry an additional static dipole moment. This implies that the site energies are correlated [65]. Dunlap et al. [66] pursued the idea further and proposed the following empirical relation for $\mu(\hat{\sigma}, F)$:

$$\mu(\hat{\sigma}_\mathrm{d}, F) = \mu_0 \exp\left(-\frac{9\hat{\sigma}_\mathrm{d}^2}{25}\right) \exp\left\{C_0\left(\hat{\sigma}_\mathrm{d}^{1.5} - \Gamma\right)\sqrt{\frac{eaF}{\sigma_\mathrm{d}}}\right\}, \tag{4}$$

where $C_0 = 0.78$, Γ describes the positional disorder, and σ_d is the width of the DOS caused by the electrostatic coupling of a charged site to neighboring dipoles. This correlated Gaussian disorder model (CGDM) explains the observed range of the $\ln \mu(F) \propto \sqrt{F}$ dependence and reproduces the $\ln \mu(F) \propto 1/T^2$ type of temperature dependence. Values for σ calculated by using (4) instead of using (3) turn out to be about 10% larger.

Equation (3) implies that the field dependence of the mobility can become negative if $\hat{\sigma} < \Sigma$ in (3a) or if $\Sigma > 1.5$ in (3b). This is a signature of positional disorder. The reason is the following. Suppose that a migrating charge carrier encounters a site from which the next jump in field direction is blocked because of poor electronic coupling. Under this condition the carrier may find it easier to circumvent that blockade. If the detour involves jumps against the field direction it

will be blocked for higher electric fields. This process involves an interplay between energetic and positional disorder and it has been treated theoretically on an advanced level [63]. The treatment supports the conceptual premise and confirms that the effect is a genuine property of hopping within an energetically and positionally disordered system rather than a signature solely of diffusion of charge carriers at low electric fields [63, 67, 68]. At very high electric fields the velocity of charge carriers must saturate and, concomitantly, $\mu(F)$ must approach a $\mu \propto 1/F$ law because jumps in a backward direction are blocked and transport becomes entirely drift-controlled. Since this effect scales with eFa/σ, the onset of saturation should occur at lower fields if the energetic disorder decreases.

3.3 Conceptual Frameworks: Polaronic Contribution to Transport

So far we have disregarded polaronic effects. However, upon ionizing a molecule or a polymer chain by adding an extra electron there is a readjustment of bond lengths because the electron distribution changes. In optical transitions this effect is revealed by the coupling of the excitation to molecular vibrations. This effect can be quantified in terms of the Huang–Rhys factor. It determines the geometric relaxation energy between the initially generated vertical Franck Condon transition and relaxed electronic state. When transferring a charge between a pair of chromophores the concomitant relaxation energy has to be transferred as well, and this implies that transport is polaronic. Unfortunately, the relaxation energy associated with placing a charge on a chromophore is not amenable to direct probing. This lack of quantitative knowledge gave rise to a lively discussion in the literature on whether or not disorder effects or polaron effects control the temperature dependence of the charge carrier mobility [69]. Meanwhile it is generally agreed that an analysis of the temperature and field dependence of the mobility solely in terms of polaronic effects requires unrealistic parameters, notably an unacceptably large electronic overlap. Moreover, polaron effects cannot explain the observation of dispersive transport at lower temperatures.

An analytical theory based upon the effective medium approach (EMA) has been developed by Fishchuk et al. [70]. They consider the superposition of disorder and polaron effects and treat the elementary charge transfer process at moderate to high temperatures in terms of symmetric Marcus rates instead of Miller–Abrahams rates (see below). The predicted temperature and field dependence of the mobility is

$$\mu = \mu_0 \exp\left(-\frac{E_a}{kT} - \frac{\hat{\sigma}}{8q^2}\right) \exp\left(\frac{\hat{\sigma}^{1.5}}{2\sqrt{2}q^2}\sqrt{\frac{eaE}{\sigma}}\right) \exp\left(\frac{eaE}{4q^2kT}\right), \tag{5}$$

where E_a is half of the polaron binding energy, $q = \sqrt{1 - \sigma^2/8eakT}$. Note that in deriving this equation, site correlations have been included. Equation (5) agrees

qualitatively with the empirical expression (6) derived from computer simulations [71]:

$$\mu = \mu_0 \exp\left(-\frac{E_a}{kT} - 0.31\hat{\sigma}^2\right)\exp\left(0.78(\hat{\sigma}^{1.5} - 1.75)\sqrt{\frac{eaE}{\sigma}}\right). \quad (6)$$

These expressions have been successfully applied to polymeric systems of practical relevance, as detailed in the next section.

3.4 Survey of Representative Experimental Results

3.4.1 On the Origin of Energetic Disorder

Although most of the recent results on charge transport in organic solids have been obtained on π-conjugated polymers and oligomers used in organic OLEDs, FETs, and PV cells, it is appropriate to refer to a recent survey on charge transport in molecularly doped polymers by Schein and Tyutnev [72]. In fact, the prime intention to develop the Gaussian disorder model has been to understand charge transport in photoreceptors used in electrophotography. This survey elaborates on the origin of the energetic disorder parameter. It has been a straightforward assumption that the disorder parameter σ is a measure of the statistical spread of the electronic interaction of a charged transport molecule with induced dipole moments in the molecular environment, i.e., the van der Waals coupling, and of the interaction between permanent dipoles of both matrix and transport molecules. By measuring the temperature dependence of the charge mobility, it has been experimentally verified that in a sample in which hole transport is carried by 1,1-bis(di-4-tolylaminophenyl)cyclohexane (TAPC) molecules, whose dipole moment is small (about 1 D), the disorder parameter increases when the polarity of its surroundings increases. This occurs for example in the order of bulk film, TAPC blended with a polar polystyrene and TAPC blended with polycarbonate in which the carbonyl groups carry a high dipole moment [73]. This proves that the polarity of the matrix increases the energetic disorder. It is straightforward to conjecture that this increase of σ is of intermolecular origin and arises from the electrostatic coupling between the charged transport unit and the statistically oriented dipole moments of the carbonyl groups.

However, in that survey Schein and Tyutnev question the intermolecular origin of σ. They compared σ values derived from studies of hole transport in 1-phenyl-3-((diethylamino)styryl)-5-(*p*-(diethylamino)phenyl)pyrazoline (DEASP) molecules, derivatives of pyrazoline, whose dipole moment is 4.34 D, blended with either polystyrene or polycarbonate as function of concentration. They found that σ is independent of the matrix material and that σ remains constant when the concentration of DEASP increases from 10% to 70% while one would expect that σ increases as

the concentration of the polar DEASP molecules increases. However, this expectation rests upon the assumption that the blend is homogeneous. It ignores aggregation effects that are particularly important for polar molecules. Since charge carriers will preferentially jump among nearest neighbor sites, dilution will only reduce the number of the transports paths between DEASP clusters rather than decreasing the ensemble averaged mean electronic coupling while the width of the DOS remains constant. Note, however, when the transport moieties are not rigid there can, in fact, be an intramolecular contribution to energetic disorder caused by a statistical distribution of conformations that translates into a spread of site energies [18].

In conjugated polymers there is an additional intra-chain contribution to the energetic disorder because the effective conjugation length of the entities that control the electronic properties is a statistical quantity. It turns out that the low energy tail of the absorption spectra as well as the high energy wing of the photoluminescence spectra can be fitted well to Gaussian envelope functions and their variances contain both intrachain and interchain contributions. Since the inhomogeneous line broadening of excitons and charge states has a common origin, it is a plausible assumption that the DOS of charge carriers in conjugated polymers is also a Gaussian, at least its low energy wing that is relevant for charge carrier hopping. Unfortunately, the DOS distribution for charge carriers is not amenable to absorption spectroscopy (see above). Indirect information can be inferred from that analysis of the temperature and field dependence of the charge carrier mobility and the shape of time of flight (ToF) signals. Note that if the DOS had an exponential rather than Gaussian tail a ToF signal would always be dispersive because charge carriers can never attain quasi equilibrium [74, 75].

3.4.2 Application of the Gaussian Disorder Model

A textbook example for the application of the uncorrelated GDM is the recent study by Gambino et al. on a light emitting dendrimer [49]. The system consists of a bis (fluorene) core, meta-linked biphenyl dendrons, and ethylhexyloxy surface units. ToF experiments shown in Fig. 5 were performed on 300 nm thick sandwich films

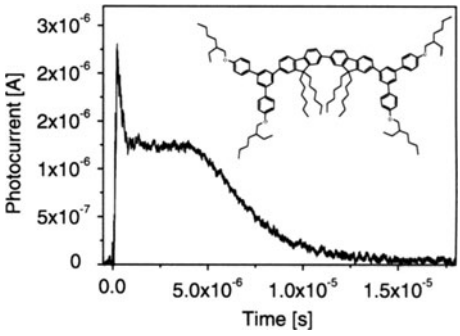

Fig. 5 Typical room temperature TOF hole transient for a first generation bis-fluorene dendrimer film of thickness 300 nm and an electric field of 1.6×10^5 V/cm. Also shown is the structure of the dendrimer. From [49] with permission. Copyright (2008) by Elsevier

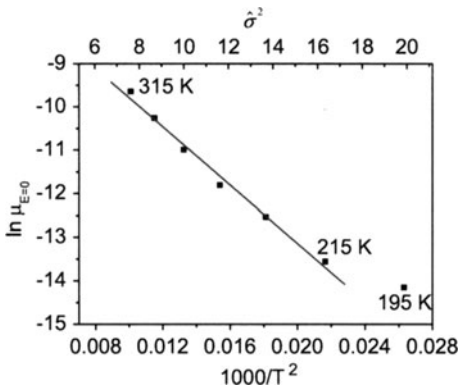

Fig. 6 Zero field hole mobility of the bis-fluorene dendrimer of Fig. 5 as a function of $1/T^2$. The deviation of the $\ln\mu(F)\propto 1/T^2$ dependence below 215 K is a signature of the onset of transit time dispersion. From [49] with permission. Copyright (2008) by Elsevier

within a temperature range between 315 and 195 K and within a field range between 1.5×10^4 and 3×10^5 V/cm using dye-sensitized injection (see Sect. 3.1). Data analysis yields an energetic disorder parameter $\sigma = 74 \pm 4$ meV, a positional disorder parameter $\Sigma = 2.6$ and $\mu_0 = 1.6 \times 10^{-3}$ cm^2 V^{-1} s^{-1}. Previous Monte Carlo simulations predicted that above a critical value of σ/kT ToF signals should become dispersive, indicating that charge carriers can no longer equilibrate energetically before they recombine with the electrode. For $\sigma = 74$ meV and a sample thickness of 300 nm the critical temperature is predicted to be 228 K. In fact, the experimental ToF signals lose their inflection points, i.e., become dispersive, at 215 K, as shown in Fig. 6. This a gratifying confirmation of the model.

Martens et al. inferred hole mobilities as a function of temperature and electric field in 100–300 nm thick films of four poly(*p*-phenylenevinylene) derivatives from space-charge-limited steady state currents injected from an ITO anode [76]. Within a dynamic range of two to three orders of magnitude the T-dependence of μ obeyed a ln μ vs T^{-2} dependence with σ values ranging from 93 meV (OC_1C_{10}-PPV) to 121 meV (partially conjugated OC_1C_{10}-PPV). In view of the extended range of the $\ln\mu$ vs $\sqrt{F}$ dependence, the data have been analyzed in terms of the correlated GMD model. Note that in their analysis the authors used a Poole–Frenkel-type of field dependence in Child's law for space-charge-limited current flow, $j_{\text{Child}} = \frac{9}{8}\frac{\varepsilon\varepsilon_0\mu F^2}{d}$. In this approach, the authors do not consider the modification of the mobility due to filling of tail states in the DOS (see Sect. 4.1). However, this modification to Child's law is only justified if the field dependence of μ is weak since a field dependent mobility has a feedback on the spatial distribution of the space charge [77, 78]. Under these circumstances there is no explicit solution for $j_{\text{Child}}(F)$ under space-charge-limited conditions [79]. However, the essential conclusion relates to the absolute value of the hole mobility and the verification of the predicted temperature dependence. The results confirm the notion that the molecular structure has an important bearing on charge transport. Broken conjugation limits transport, mainly due to the effective dilution of the fraction of the charge transporting moieties as evidenced by the low value of the prefactor to the mobility $\mu_0 = 4 \times 10^{-6}$ cm^2 V^{-1} s^{-1}. This prefactor is a measure of the electronic coupling among the

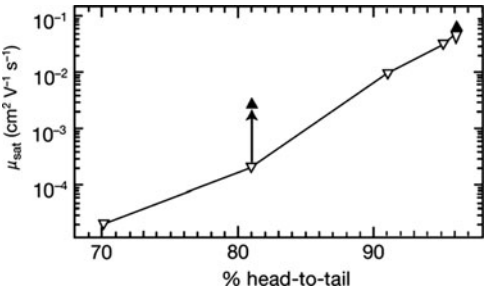

Fig. 7 Room temperature FET-mobility of P3HT in different microstructures. *Downward triangles*: spin-coated regioregular film, *upward triangles*: solution cast film. From [83] with permission. Copyright (1999) by Macmillan Publishers

transport sites. In this respect, bulky transport groups containing spiro-units are unfavorable [80, 81]. On the other hand, sterically demanding groups reduce charge trapping because they diminish the propensity of the sites for forming sandwich conformations that can act as charge carrier traps. Using a polymer with a high degree of regioregularity can significantly increase the mobility due to improved electronic interchain coupling and decreasing energetic disorder. Improved inter-chain ordering in substituted poly(3-hexylthiophene) (P3HT) can raise mobility up to 0.1 $cm^2\ V^{-1}\ s^{-1}$ [82, 83] as demonstrated in Fig. 7. The impact of this inter-chain ordering is also revealed in optical spectroscopy [84, 85]. This effect is profitably used in organic FETs and organic integrated circuits, employing, for instance ordered semiconducting self-assembled monolayers on polymeric surfaces. Such systems can be exploited in flexible monolayer electronics. Surprisingly, in the ladder-type poly-phenylene (MeLPPP), which is one of the least disordered of all π-conjugated polymers, the hole mobility is only about 3×10^{-3} $cm^2\ V^{-1}\ s^{-1}$ at room temperature [36]. Since the temperature dependence is low – because of low disorder – this has to be accounted for by weak inter-chain interactions. Obviously, the bulky substituents reduce the electronic coupling among the polymer chains.

Despite the success of the disorder model concerning the interpretation of data on the temperature and field dependence of the mobility, one has to recognize that the temperature regime available for data analysis is quite restricted. Therefore it is often difficult to decide if a $\ln \mu$ vs T^{-2} or rather a $\ln \mu$ vs T^{-1} representation is more appropriate. This ambiguity is an inherent conceptual problem because in organic semiconductors there is, inevitably, a superposition of disorder and polaron effects whose mutual contributions depend on the kind of material. A few representative studies may suffice to illustrate the intricacies involved when analyzing experimental results. They deal with polyfluorene copolymers, arylamine-containing polyfluorene copolymers, and σ-bonded polysilanes.

3.4.3 Polaronic Effects vs Disorder Effects

The most comprehensive study is that of Khan et al. [86]. They describe ToF experiments on sandwich-type samples with films of poly(9,9-dioctyl-fluorene)

(PFO), PFB, and a series of fluorene-triarylamine copolymers with different triarylamine content covering a broad temperature and field range. In all cases the field dependence of the hole mobility follows a $\ln \mu \propto \sqrt{F}$ dependence and a super-Arrhenius-type of temperature dependence. At lower temperatures the ToF signals are dispersive. When analyzing the experimental data the authors first checked whether or not the uncorrelated Gaussian disorder model (GDM) is appropriate. There are indeed reasonably good fits to the temperature and field dependence based upon (3). Recognizing, however, that experimentally observed $\ln \mu$ vs $\sqrt{F}$ dependence extends to lower fields than the GDM predicts, they went one step further and tested the correlated disorder model (CDM) in the empirical form of (4). Here the site separation enters as an explicit parameter. This analysis confirms the validity of the $\ln \mu \propto T^{-2}$ law except that the σ values turn out to be 10% larger because in the CDM the coefficient that enters the exponent in the temperature dependence is 3/5 instead of 2/3 in the GDM. The positional disorder parameters are comparable and the values for the site separation are realistic. Finally the authors took into account polaron effects by using the empirical expression (6). The difficulty is how to separate the polaron and disorder contributions to the T-dependence of μ. This can be done via an analysis of the field dependence of μ. Once σ is known the factor $\exp\left(-\frac{E_a}{kT}\right)$, that accounts for the polaron contribution, can be determined. The parameters inferred from the data fits are then compared by Khan and coworkers [86]. They find that by taking into account polaronic contributions, the σ value decreases while the prefactor to the mobilities increases by roughly one order of magnitude. The polaron binding energy $2E_a$ is significant and ranges between 0.25 eV and 0.40 eV: Nevertheless, energetic disorder plays a dominant role in hole transport. It is larger in the copolymers as compared to the homopolymers PFO and PFB.

A similar analysis has been carried out by Kreouzis et al. for hole transport in pristine and annealed polyfluorene films [87]. Consistent with the work of Khan et al. [86] on the copolymers, the results can best be rationalized in terms of the correlated disorder model including polaron effects. For different unannealed samples σ values are between 62 and 75 meV, the polaron activation energies are 180 meV, and the prefactor mobilities μ_0 are 0.4 and 0.9 $cm^2\ V^{-1}\ s^{-1}$. Annealing reduces the disorder parameters to 52 ± 1 meV and the prefactor to 0.3 $cm^2\ V^{-1}\ s^{-1}$. It is well known that PFO can exhibit different phases [88, 89]. Annealing an amorphous PFO film induces the formation of a fraction of the so-called β-phase, where chains are locked into a planar conformation resulting in a long conjugation length and low disorder. This lowers the geometric relaxation energy upon ionization, i.e., the polaron binding energy, for the β-phase.

However, one should be cautious about overinterpreting the field and temperature dependence of the mobility obtained from ToF measurements. For instance, in the analyses of the data in [86, 87], ToF signals have been considered that are dispersive. It is well known that data collected under dispersive transport conditions carry a weaker temperature dependence because the charge carriers have not yet reached quasi-equilibrium. This contributes to an apparent Arrhenius-type temperature dependence of μ that might erroneously be accounted for by polaron effects.

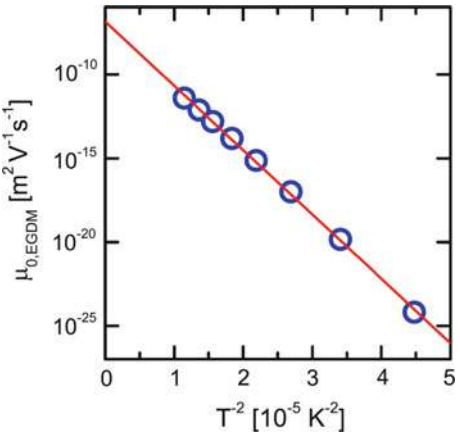

Fig. 8 Temperature dependence of the zero field hole mobility in the low carrier density limit in a polyfluorene copolymer. The data are inferred from space-charge-limited current experiments and analyzed in terms of the extended Gaussian disorder model (see Sect. 4.1). From [90] with permission. Copyright (2008) by the American Institute of Physics

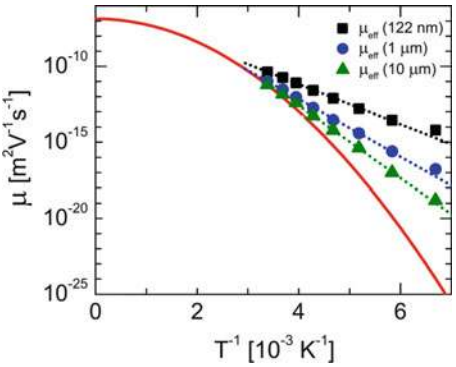

Fig. 9 Temperature dependence of the hole mobility of a polyfluorene copolymer inferred from space-charge-limited current measurements on samples of thicknesses 122 nm, 1 μm, and 10 μm. The *full curve* is an extrapolation to the low carrier density limit using the extended Gaussian disorder model. From [90] with permission. Copyright (2008) by the American Institute of Physics

In fact, in their recent work, Mensfoort et al. [90] conclude that in polyfluorene copolymers hole transport is entirely dominated by disorder. This is supported by a strictly linear $\ln \mu \propto T^{-2}$ dependence covering a dynamic range of 15 decades with a temperature range from 150 to 315 K (Fig. 8). Based upon stationary space-charge-limited current measurement, where the charge carriers are in quasi equilibrium so that dispersion effects are absent, the authors determine a width σ of the DOS for holes as large as 130 meV with negligible polaron contribution.

The work of Mensfoort et al. is a striking test of the importance of charge carrier density effects in space-charge-limited transport studies. For a given applied voltage the space charge concentration is inversely proportional to the device thickness. This explains why in Fig. 9 the deviation from the $\ln \mu \propto T^{-2}$

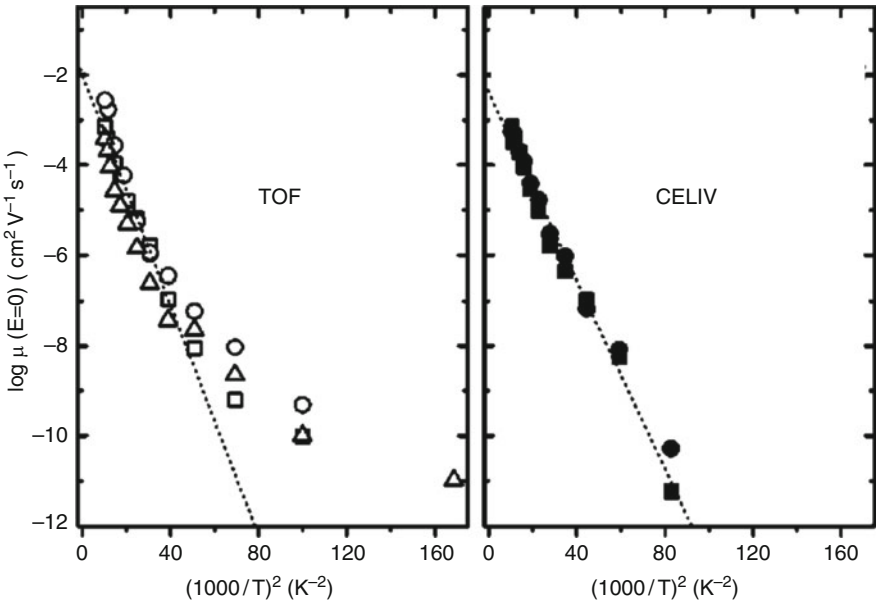

Fig. 10 Temperature dependence of the hole mobility in regioregular P3HT measured in TOF (*left*) and CELIV (*right*) configuration. *Different symbols* refer to different samples. From [91] with permission. Copyright (2005) by the American Institute of Physics

dependence of the hole mobility becomes more significant in thinner samples. This will be discussed in greater detail in Sect. 4.1.

In this context it is appropriate to recall the work of Mozer et al. [91] on hole transport in regio(3-hexylthiophene). These authors compared the field and temperature dependencies of the hole mobility measured via the ToF and CELIV methods. Quite remarkably, the temperature dependence deduced from ToF signals plotted on a $\ln \mu$ vs T^{-2} scale deviate significantly from linearity while the CELIV data follow a $\ln \mu \propto T^{-2}$ law down to lowest temperatures (180 K) (see Fig. 10). The reason is that in a ToF experiment the charge carriers are generated randomly within the DOS and relax to quasi-equilibrium in their hopping motion while in a CELIV experiment relaxation is already completed. This indicates that a deviation from a $\ln \mu \propto T^{-2}$ form may well be a signature of the onset of dispersion rather than a process that is associated with an Arrhenius-type of temperature dependence such as polaron transport. Therefore the larger polaron binding energy that had been extracted from ToF data measured in the non-annealed PFO films should be considered with caution. Obviously, if one wants to distinguish between polaron and disorder effects based upon the temperature and field dependencies of the mobility one should ensure that dispersion effects are weak.

The conclusion that polaron effects contribute only weakly to the temperature dependence of the charge carrier mobility is supported by a theoretical study of

polarons in several conjugated polymers. Meisel et al. [92] considered the electron–phonon interaction and calculated polaron formation in polythiophene, polyphenylenevinylene, and polyphenylene within an extended Holstein model. Minimization of the energy of the electronic state with respect to lattice degrees of freedom yields the polaron ground state. Input parameters of the Hamiltonian are obtained from ab initio calculations based on density-functional theory (DFT). The authors determined the size and the binding energies of the polarons as well as the lattice deformation as a function of the conjugation length. The binding energies decrease significantly with increasing conjugation length because the fractional change of bond lengths and angles decreases as the charges are more delocalized. The polaron extents are in the range of 6–11 nm for polythiophenes and polyphenylenevinylenes, and the associated polaron binding energies are 3 meV for holes and 7 meV for electrons. For polyphenylenes, the polaron size is about 2–2.5 nm and its binding energy is 30 meV for the hole and 60 meV for the electron. Although the calculations document that charge carriers are self-trapped, they indicate that polaron binding energies are much smaller than the typical width of the DOS of representative π-bonded conjugated polymers. This raises doubts on the conclusiveness of analyses of mobility data inferred from dispersive ToF signals.

Another cautionary remark relates to the field dependence of the charge carrier mobility. Ray Mohari et al. [93] measured the hole mobility in a blend of *N*,*N*′-diphenyl-*N*,*N*′-bis(3-methylphenyl)-(1,1′-biphenyl)-4,4′-diamine (TPD) and polystyrene in which the TPD molecules tend to aggregate. In the ordered regions the energetic disorder is significantly reduced relative to a system in which TPD is dispersed homogeneously. The experiments confirm that aggregation gives rise to a negative field dependence of the mobility. Associating that effect solely with positional disorder in a hypothetical homogenous system would yield a positional disorder parameter that is too large. These results demonstrate that changes of sample morphology can be of major impact on the field dependence of μ.

In the context of polaron effects we also mention the experimental work on hole transport in polysilanes that has been analyzed in terms of Fishchuk et al.'s analytical theory [70]. In this theory polaron effects are treated in Marcus terms instead of Miller–Abrahams jump rates, taking into account correlated energy disorder [see (5)]. The materials were poly(methyl(phenyl)silylene) (PMPSi) and poly(biphenyl(methyl)silylene) (PBPMSi) films. Polysilanes are preferred objects for research into polaron effects because when an electron is taken away from a σ-bonded, i.e., singly-bonded, polymer chain there ought to be a significant structural reorganization that gives rise to a comparatively large polaron binding energy. Representative plots for the temperature dependence of the hole mobility in PMPSi are shown in Fig. 11. Symbols show experimental data, full lines are theoretical fits. Considering that there is no arbitrary scaling parameter, those fits are an excellent confirmation of the theory. Note that the coupling element J that enters the Marcus rate has been inferred from the prefactor mobility. The data analysis also shows that the polaron binding energies in these materials are significant and depend on the pendant group.

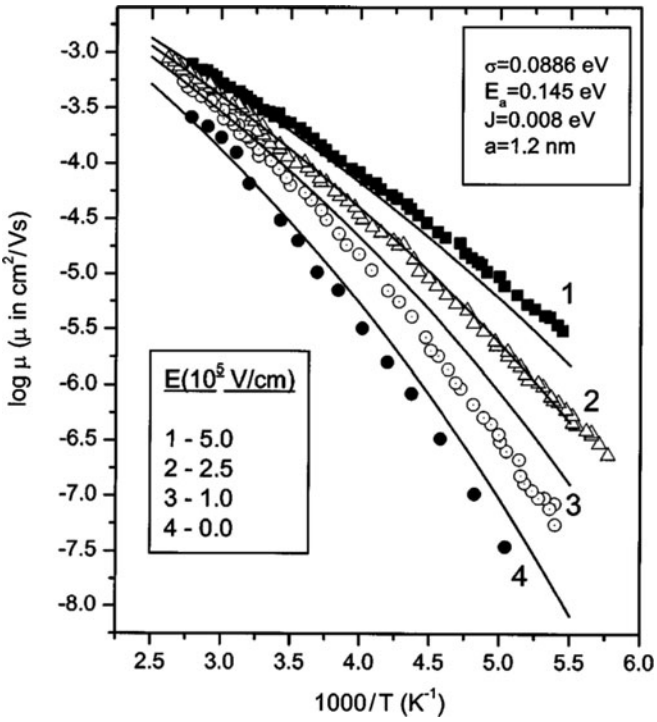

Fig. 11 Temperature dependence of the hole mobility in PMPSi at different electric fields. *Full curves* are calculated using the theory by Fishchuk et al. [70]. The fit parameters are the width σ of the density of states distribution, the activation energy E_a (which is $E_p/2$), the electronic exchange integral J, and the intersite separation a. From [70] with permission. Copyright (2003) by the American Institute of Physics

4 Charge Transport at High Carrier Density

4.1 Charge Transport in the Presence of Space Charge

The transport models discussed in Sect. 3 are premised on the condition that the interaction of the charge carriers is negligible. This is no longer granted if (1) a trapped space charge distorts the distribution of the electric field inside the dielectric, (2) ionized dopant molecules modify the DOS, or (3) the current flowing through the dielectric is sufficiently large so that a non-negligible fraction of tail states of the DOS is already occupied. The latter case is realized when either the current device is space-charge-limited (SCL) or the current is confined to a thin layer of the dielectric, for instance in a field effect transistor. It is conceptionally easy to understand that the temperature dependence of the charge carrier mobility must change when charge carriers fill up tail states of the DOS beyond the critical level defined by the condition of quasi-equilibrium. In this case the carrier statistics

becomes Fermi–Dirac-like whereas it is Boltzmann-like if state filling is negligible. At low carrier density, a charge carrier in thermal equilibrium will relax to an energy $\varepsilon_\infty = \frac{\sigma^2}{kT}$ below the center of the DOS, provided it is given enough time to complete the relaxation process. Charge transport, however, requires a certain minimum energy to ensure there are enough neighboring sites that are energetically accessible [54]. To reach this so-called transport energy from the thermal equilibrium energy, an activation energy is needed. If, at higher carrier density, a quasi-Fermi level will be established that moves beyond ε_∞, the activation energy needed for a charge carrier to reach the transport level decreases and, concomitantly, the mobility increases (Fig. 12). This is associated not only with a weaker temperature dependence of μ but also with a gradual change from the $\ln \mu \propto T^{-2}$ dependence to an Arrhenius-type $\ln \mu \propto T^{-1}$ dependence because upward jumps of charge carriers no longer start from a temperature dependent occupational DOS but from the Fermi-level set by the applied voltage. The straightforward verification of this effect is the observation that the carrier mobilities measured under FET-conditions can be up to three orders of magnitude larger than the values inferred from ToF experiments [94]. Further, one observes a steeper increase of space-charge-limited current mobility with electric field than predicted by Child's law [76]. It is meanwhile recognized that this steeper increase is not due to a field dependence of the mobility under the premise of negligible concentration. Rather, as illustrated by Fig. 13, it is mostly an effect of the filling up of the DOS due to the increase of the

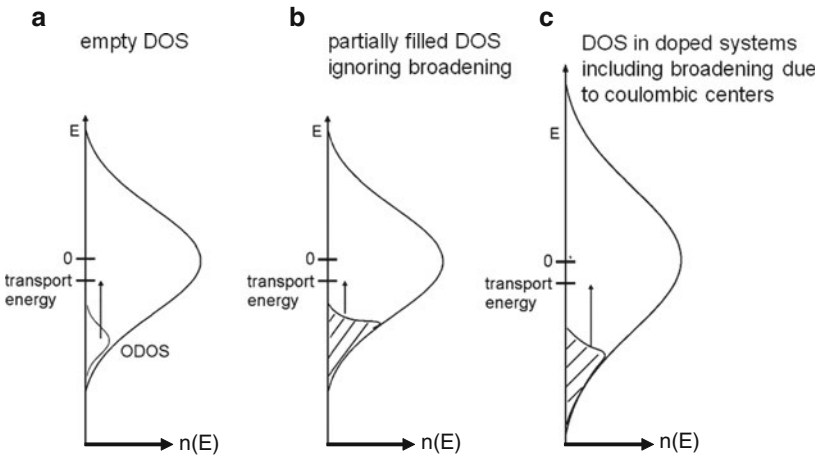

Fig. 12 Schematic view of the effect of state filling in the Gaussian distribution of the hopping states. (**a**) Charge carrier transport requires thermally activated transitions of a charge carrier from the occupational DOS (ODOS) to the transport energy E_{tr} in the low carrier limit. (**b**) Charge transport in the presence of a space charge obeying Fermi–Dirac statistics under the assumption that the space charge does not alter the DOS. (**c**) Charge transport in the presence of a space charge considering the broadening of the DOS due the countercharges generated, e.g., in the course of electrochemical doping. Note the larger width of the DOS

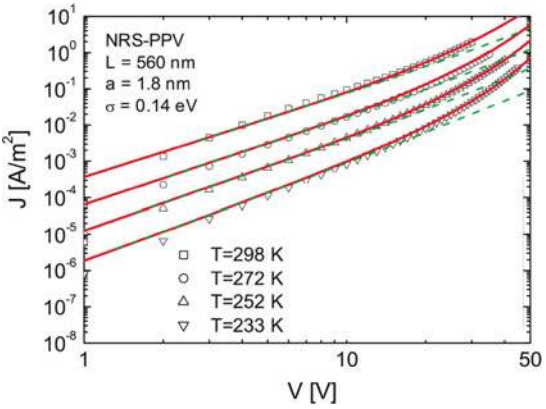

Fig. 13 Experimental (*symbols*) and theoretical (*lines*) data for the current-density as a function of applied voltage for a polymer film of a derivative of PPV under the condition of space-charge-limited current flow. *Full curves* are the solution of a transport equation that includes DOS filling (see text), *dashed lines* show the prediction of Child's law for space-charge-limited current flow assuming a constant charge carrier mobility. From [96] with permission. Copyright (2005) by the American Institute of Physics

charge carrier concentration [95]. Ignoring this effect in a data analysis would yield numerically incorrect results.

Among the first theoretical treatments of transport in the presence of a space charge is that of Arkhipov et al. [97]. These authors pointed out that in chemically doped materials and in the conduction channel of an FET the number of charge carriers occupying deep tail states of the Gaussian DOS can be significant relative to the total density of states. They developed a stochastic hopping theory based upon the variable range concept and incorporated the Fermi–Dirac distribution to describe the temperature dependence of the mobility. Currently the most frequently used formalism is that of Pasveer et al. [96]. It is based upon a numerical solution of the master equation representing charge carrier hopping in a lattice. Considering that a fraction of sites is already occupied, charge transport is considered as a thermally assisted tunneling process with Miller–Abrahams rates in a Gaussian manifold of states with variance σ, tacitly assuming that formation of a bipolaron, i.e., a pair of like charges on a given site, is prevented by coulomb repulsion. The results can be condensed into an analytical solution in factorized form,

$$\mu(T, F, n) = \mu_0(T) g_1(F, T) g_2(n), \tag{7}$$

where $\mu_0(T)$ is the temperature dependent mobility in the limit of $F = 0$, $g_1(F, T)$ is the mobility enhancement due to the electric field, and $g_2(n)$ is the enhancement factor due to state filling.

A more comprehensive theoretical treatment has been developed by Coehoorn et al. [98] in which the various approaches for charge carrier hopping in random organic systems have been compared. In subsequent work, Coehoorn [99] used two

semi-analytical models to focus on charge transport in host guest systems, namely a relatively simple Mott-type model and a more advanced effective medium model. The latter model was generalized in order to be able to include the effect of different wave function extensions of host and guest molecules in a blend system.

At the same time Fishchuk et al. [100] developed an analytical theory based upon the effective medium approach to charge transport as a function of the charge carrier concentration within the DOS. In contrast to the work by Pasveer et al. they included polaron effects. It is obvious that how charges are transported, i.e., the trade-off between disorder and polaron effects, should have a major impact on the result. In the extreme case of vanishing disorder yet strong polaronic coupling, filling tail states of DOS by charge carriers should not have an effect on the transport except at very large charge concentration when coulomb repulsion becomes important. Filling-up tail states of the DOS will, however, become progressively important as the disorder contribution to charge transport increases. To incorporate polaron effects, Fishchuk et al. [100] replaced the Miller–Abrahams-type of hopping rate with a Marcus rate. Note, however, that the magnitude of the effect of DOS filling is solely determined by the ratio between the disorder energy σ and the polaron energy E_p and not by the analytical form of the hopping rate. The prize for doing analytical rather than numeric work is that it requires the solving of integrals of the hopping rate over the density of states in an effective medium approach, thus yielding a rather complicated expression. It is gratifying, though, that both the treatments of Arkhipov et al. and Pasveer et al. as well as Fishchuk et al.'s effective medium approach (EMA) are mutually consistent [96, 97, 100]. Figure 14 compares the results of the three models as a function of carrier concentration parametric in the disorder parameter σ. Figure 15 demonstrates that the effective medium approach provides a good fit to the concentration dependence of the carrier mobility in field effect transistors (FETs) using P3HT and OC_1C_{10}-PPV as active layers while Fig. 16 shows the temperature dependence of $\ln \mu$ vs T^{-1} and $\ln \mu$ vs T^{-2} parametric in the carrier concentration. It is obvious that there is a transition from the $\ln \mu \propto T^{-2}$ dependence at $n = 0$ to a $\ln \mu \propto T^{-1}$ law at higher concentrations. The Fishchuk et al. theory also confirms that, in a system in which polaron effects are dominant, $E_a/\sigma = 3$ implying $E_p/\sigma = 6$, i.e., the temperature dependence of the transport is dominated by polaron effects instead of disorder, so that the filling of the DOS with carrier density is unimportant. Unfortunately, the present EMA treatment does not allow encompassing of the parameter regime $E_a/\sigma < 3$.

Recently, Fishchuk et al. extended their effective medium approach to include a discussion of the so-called Meyer Neldel rule [102]. The Meyer Neldel rule is an empirical relation, originally derived from chemical kinetics. It describes the fact that enthalpy and entropy of a chemical reaction are functionally related to each other. More generally, it states that in a thermally activated rate process an increase in the activation energy needed is partially compensated by an increase in the prefactor. There are numerous examples, notably in semiconductor physics, that this rule is fulfilled for various reasons. Recently Emin advanced an adiabatic polaron hopping model that considers carrier-induced softening of the vibrations promoting charge carrier motion [103]. Fishchuk et al. were able to show that in

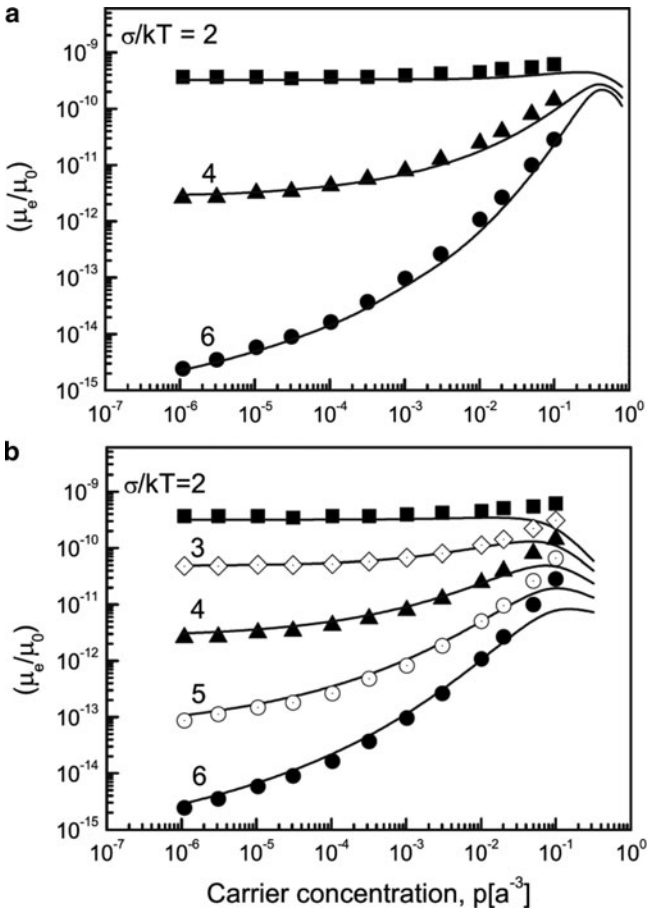

Fig. 14 A comparison of different approaches to describe the charge carrier mobility in a Gaussian-type hopping system as a function of the normalized concentration of the charge carriers. (**a**) *Full curves* are the result of effective medium calculations [100] while *symbols* are computer simulations [96]. (**b**) *Full curves* are calculated using the variable range hopping concept [101], *symbols* are the computer simulations. From [100] with permission. Copyright (2007) by the American Institute of Physics

a disordered system with a partially filled density of states distribution the Meyer–Nedel rule is indeed fulfilled but it is not related to polaronic transport. Instead, it is a genuine signature of hopping transport in a random system with Gaussian DOS distribution upon varying the charge carrier concentration as realized, e.g., in a field effect transistor at variable gate voltage. Figure 17 shows the temperature dependence of the hole mobility measured in a field effect transistor (FET) with pentacene (Fig. 17a) and P3HT (Fig. 17b) as active layers. This study also disproves the previous claim by Craciun et al. [104] that the temperature dependence of the charge carrier mobility in a variety of conjugated polymers

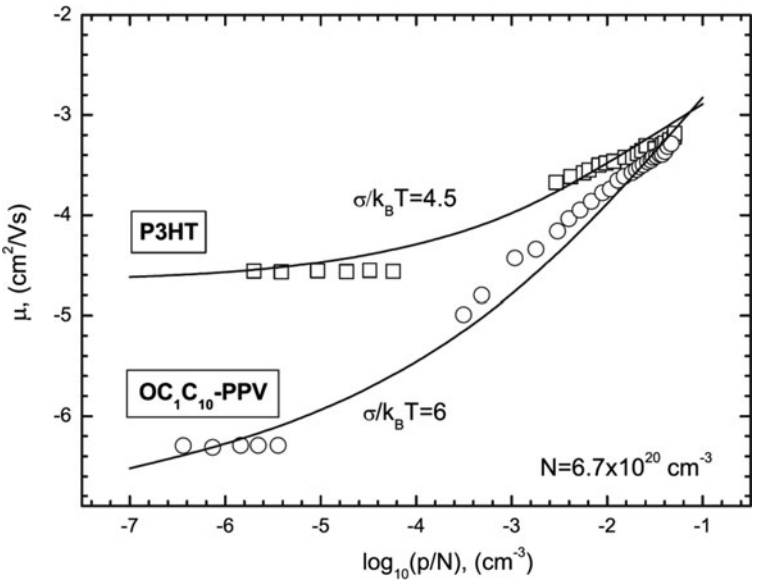

Fig. 15 Fits to experimental values of the hole FET-mobility using P3HT and OC_1C_{10}-PPV as active layers. From [100] with permission. Copyright (2007) by the American Institute of Physics

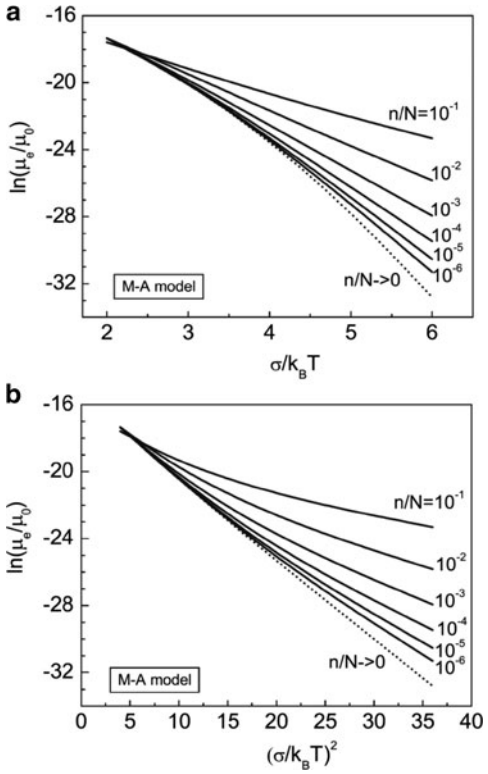

Fig. 16 Calculated charge carrier mobility in a Gaussian-type hopping system parametric in the charge carrier concentration and plotted (**a**) on a ln μ vs σ/kT scale and (**b**) on a ln μ vs $(\sigma/kT)^2$ scale. From [100] with permission. Copyright (2007) by the American Institute of Physics

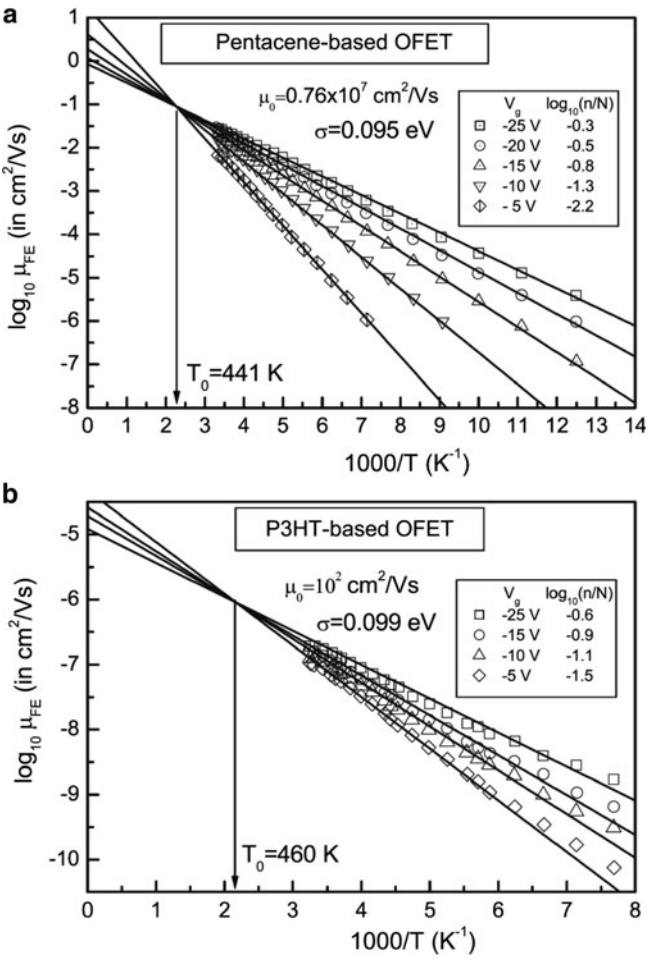

Fig. 17 Temperature dependence of the hole mobility measured in an FET with (**a**) pentacene and (**b**) P3HT as active layers. Parameter is the gate voltage. Data fitting using the Fishchuk et al. theory in [102] yields values for the mobility and the disorder potential extrapolated to zero electric field and zero carrier concentration. T_0 is the Meyer–Nedel temperature (see text). From [102] with permission. Copyright (2010) by the American Institute of Physics

extrapolates to an universal value of 30 $cm^2\ V^{-1}\ s^{-1}$ in the $T \rightarrow \infty$ limit. This has been corroborated by the work of Mensfoort et al. (see Fig. 9).

Meanwhile the Pasveer et al. formalism [96] has been termed as "extended Gaussian disorder model (EDGM)" and "extended correlated disorder model (ECDM)" depending on whether the correlation of the site energies is included or not. The EGDM has recently been applied to analyze the SCL current injected from an ohmic PEDOT:PSS anode into a polyfluorene based light emitting polymer layer with different layer thicknesses [105]. It is instructive to compare the experimental

current–voltage characteristics to curves calculated by using the classic Child's law combined with a Poole–Frenkel-type field dependence of the mobility to the predictions of the EGDM model in which DOS filling has been taken into account. The comparison indicates that (1) the EGDM model can reproduce the experimental results with remarkable accuracy, yet (2) high precision regarding data quality is required to distinguish among the various models, and (3) the influence of DOS filling diminishes in thicker samples. The latter effect results from the inverse decay of the carrier concentration with cell thickness at constant applied electric field. This may explain why Agrawal et al. [106] could successfully explain their SCL current flow in copper phthalocyanine (CuPc) layers with thicknesses ranging from 100 to 400 nm. The same reasoning applies to the work of Mensfoort et al. [90] on SCL current flow in the polyfluorene diode mentioned above. The authors demonstrate that in a thick sample the temperature dependence of the mobility strictly follows a $\ln \mu \propto T^{-2}$ law yet it acquires a $\ln \mu \propto T^{-1}$ branch at lower temperatures with an activation energy that decreases with decreasing layer thickness. At lower temperatures, a Fermi level is formed at an energetic position that depends on the carrier concentration and thus on the film thickness. Their quantitative data analysis confirms the notion that in this material polaron effects are unimportant. This is consistent with the work of Meisel et al. [92].

4.2 Transport in Doped Semiconductors

The conventional way to increase the conductivity of a semiconductor is to introduce dopants that can act as electron donors or/and acceptors. In fact, significant progress with inorganic semiconductors could only be obtained once carrier transport was no longer determined by impurities but could be controlled and tuned by doping. Controlled and stable doping can be accomplished easily in inorganic semiconductors yet it imposes serious problems for organic semiconductors. The problem is related to the level spectrum of transport states. P-type doping requires the transfer of an electron from the filled HOMO of the host to the LUMO of the dopant at no or only little energy expense as illustrated in Fig. 18.

Correspondingly, the HOMO of the dopant has to be close to the LUMO of the host in order to promote n-type doping. This puts serious constraints on the mutual energy levels. In most organic materials the HOMO is around -5 to -6 eV below the vacuum level. Assuming an electrical bandgap of 2.5 eV, a p-type dopant therefore has to act as a very strong electron acceptor. N-type dopants had to have a HOMO level near -2.5 to -3.5 eV. Clearly, this is difficult to achieve. On the other hand, it would be of considerable advantage to be able to raise the concentration of mobile charge carriers significantly. In addition to yielding a higher carrier mobility, as outlined above, a higher charge carrier density should also reduce ohmic losses at internal interfaces. Note that in organic semiconductors the intrinsic conductivity is low. Therefore a device behaves like a dielectric medium, and an applied voltage drops across the bulk of the sample rather than at

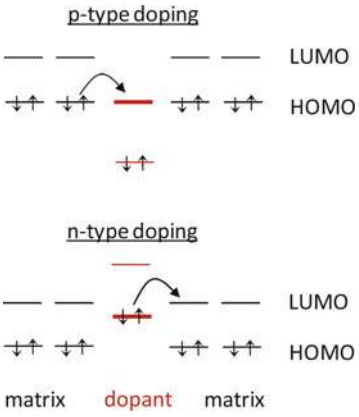

Fig. 18 Doping mechanisms for molecular p-type doping (*top*) and for n-type doping (*bottom*). P-type (n-type) doping is achieved when the molecular dopant acts as acceptor (donor). After [107]

an active interfacial layer between, say, donor and acceptor layers. If one were to increase the conductivity of the material, in which the charge carriers are transported towards the interfacial layer by doping, one would ensure that a larger fraction of the applied voltage drops at the active layer. Therefore doping should minimize ohmic losses.

Attempts to dope organic semiconductors have been made very early in the field, motivated by the prospect of possibly reaching metallic conductivities [108, 109]. These "synthetic metals," however, have not been realized. While p-type doping could be obtained, for example, with iodine gases for poly-*p*-phenylene vinylene (PPV) derivatives, and n-type doping was demonstrated with sodium for a cyano-derivative of PPV, the doping levels obtained were not stable with time. The dopant molecules readily diffused into the organic semiconductor, yet also out of it. Due to the lack of stability, these approaches were not suitable for commercial applications.

Pioneering work on *stable* doping in organic LEDs has been carried out by the group of K. Leo in Dresden and has been reviewed by Walzer [107]. It is now clear that F_4-TCNQ can act as a dopant because its electron affinity is close to 5 eV [110, 111], which is close to the ionization potential of triphenylamine derivatives and to some phthalocyanines (Pc) [107]. It turns out that doping of ZnPc by 2% of F_4-TCNQ raises the conductivity to a level of $10^{-3}\ \Omega^{-1}\ \mathrm{cm}^{-1}$. When using TCNQ instead of F_4-TCNQ the conductivity is only $10^{-6}\ \Omega^{-1}\ \mathrm{cm}^{-1}$. This illustrates the importance of the fluoro-substituents that raise the electron affinity. After all, the key parameter for efficient p-type doping is the difference between the LUMO of the dopant and the HOMO of the host [112, 113], although some level mismatch can be compensated by the effect of disorder broadening of the distribution of transport states. One can expect that disorder ameliorates a fatal level mismatch in a similar way as it is the case of thermally activated charge injection from an electrode (see Sect. 6).

The concentration of free holes generated by the p-dopant can be calculated under the assumption that doping does not alter the hole mobility. Doing so, Zhang

et al. [114] derived a concentration of free holes of 4×10^{16} cm^{-3} upon doping a PPV film by F_4-TCNQ at a doping ratio of 1:600. At such a doping level processable films are still formed. By relating the charge concentration to the mass ratio the authors estimated that only 1% of the dopant molecules are ionized. This is supported by impedance spectroscopy on Schottky diodes. However, the assumption of a constant mobility is not trivial. There is a superposition of several conceivably compensating effects including level filling (see below), DOS broadening (see below), charge percolation, and changes of the wavefunction overlap parameter that controls charge carrier hopping [115].

In contrast to p-type doping, n-type doping is intrinsically much more difficult to achieve because dopants with high lying HOMO levels can easily and inadvertently be reduced by oxygen. One way towards n-type doping is the use of alkali metals such as lithium or cesium [107]. They are frequently employed to improve electron injection from the anode of an OLED [116]. In small molecule OLED devices, fabricated by evaporation, the dopant metal can be coevaporated. Replacing lithium by cesium has the advantage that Cs^+ ions have a lower diffusivity compared to the small Li^+ ions. This makes the devices less sensitive to temperature and helps keep the dopant away from the charge recombination layer. This is important because ion diffusion into the recombination zone causes quenching of the electroluminescence.

A first study of controlled molecular n-type doping in molecular organic semiconductors was presented by Nollau et al. [117]. They doped naphthalene-tetracarboxylic dianhydride (NTCDA) by co-sublimation with the donor molecule bis(ethylenedithio)-tetrathiafulvalene. It was shown that the Fermi level shifts towards the transport level and that the conductivity was increases. However, the conductivities achieved were rather low and only one to two orders of magnitude above the background conductivity of nominally undoped NTCDA. More successful was doping of hexadecafluorophthalocyaninatozinc (F_{16}ZnPC) by tetrathianaphthacene (TTN). The dependence of the UPS spectra on doping suggested that TTN acts as an efficient donor. Essentially no doping was found with Alq_3 as a host material because its LUMO is too high to allow for efficient electron injection from TTN [118]. Another pair of host and guest materials, investigated by the Kahn group [119], is an electron transporting tris(thieno)hexaazatriphenylene derivative doped with bis(cyclopentadienyl)-cobalt(II) that has an unusually low ionization energy of 4 eV in the condensed phase. By UV, X-ray, and inverse photoemission studies the authors concluded that the dopant shifts the Fermi level 0.56 eV towards the unoccupied states of the host. A three orders of magnitude increase in the current was demonstrated. The result indicates that the electron is still quite localized at the dopant site and requires thermal activation for complete ionization.

Another way to accomplish n-type doping is by using cationic dyes [120, 121]. The cationic doping method has been applied successfully for solar cells in which materials with low lying LUMOs are used for electron transporting purposes. The straightforward message is that one has to employ strong electron acceptors as hole transporters, since the HOMO of a stable n-type dopant cannot be higher than, say,

4 eV. Of course, there is a price to pay for this because the lower the LUMO of the hole acceptor the more likely it is that an impurity acts as a hole trap and vice versa.

In the case of doping by organic salts one should be aware of the effects caused by the inevitable presence of counter ions. They act as coulomb wells and modify the DOS of the transport states. By fabricating a gated electrochemical cell with PPV as a transporting film and Au/Pt as source-drain electrodes immersed in an electrolyte (0.1 M tetrabutylammonium perchlorate or hexafluorophosphate or $LiClO_4$ in acetonitrile) Hulea et al. were able to quantify this effect [122]. When the applied potential is increased, holes are injected into PPV. Their charge is counterbalanced by ClO_4^- or PF_6^- ions that enter the film from the electrolyte. The number of holes, inferred from the differential capacitance, allows the energy spectrum of transport states (DOS) to be mapped out. The resulting DOS carries a Gaussian core centered at 5.55 ± 0.02 eV with a variance of 0.19 ± 0.01 eV followed by an exponential tail. However, at very low doping, 10^{-4} (states/eV) per monomer, the DOS is a single Gaussian with variance of 0.11 eV. This is consistent with charge transport studies on an undoped film [123]. Obviously, the presence of random coulomb centers broadens the Gaussian distribution and creates deep tail states, in corroboration of earlier Monte Carlo simulations [124] and more recent analytical theory [125]. The broadening of the tail states is illustrated in Fig. 19. The net effect of this tail broadening is a decreasing charge carrier mobility at low to moderate doping levels. At higher doping levels the coulomb traps overlap spatially and smooth the energy landscape. A striking documentation of this effect

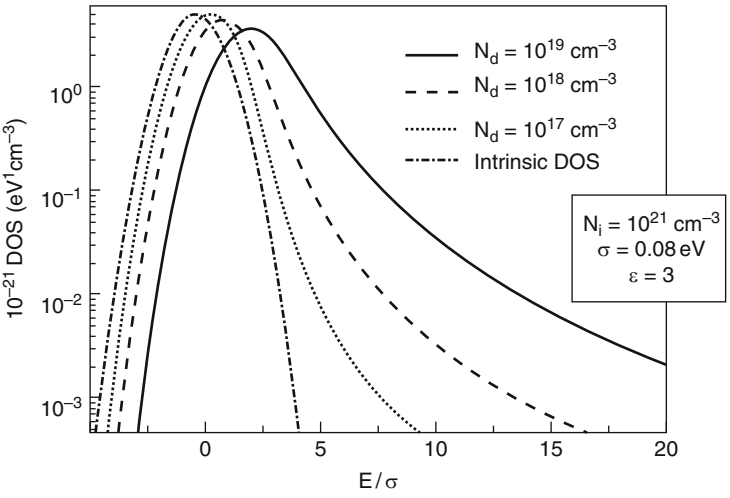

Fig. 19 The effect of doping on the density of states distribution in a disordered organic semiconductor at variable concentration of charged dopants. The energy scale is normalized to the width of the DOS, expressed through σ, of the undoped sample. The parameters are the intrinsic site concentration N_i and the dopant concentration N_d. From [125] with permission. Copyright (2005) by the American Institute of Physics

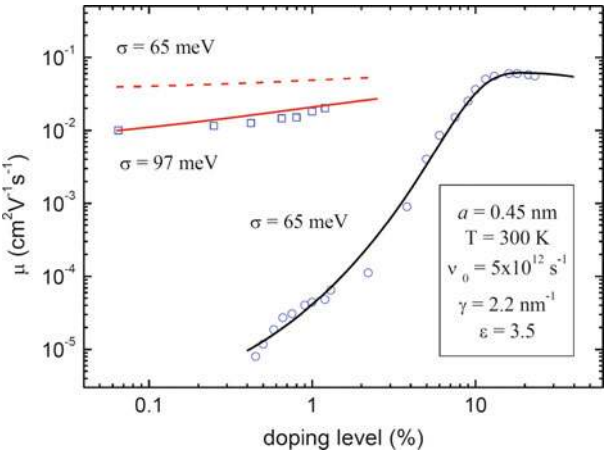

Fig. 20 Charge carrier mobility in P3HT as a function of the charge carrier concentration. *Squares* refer to an experiment performed on a field effect transistor while *circles* refer to experiments done on an electrochemically doped sample. In the latter case the mobility is inferred from the steady state current at a given doping level. *Solid* and *dashed lines* have been fitted using the theory of [101]. The fit parameters are the site separation a, the prefactor v_0 in the Miller–Abrahams-type hopping rate, the inverse wavefunction decay parameter γ and the dielectric constant ε. From [101] with permission. Copyright (2005) by the American Institute of Physics

is presented in Fig. 20. It shows the dependence of the hole mobility in a P3HT film as a function of concentration of holes generated either by electrochemical doping or by injection from electrodes in an FET structure. In the former case the counter charges are ions incorporated within the film while in the latter they are weakly bound electrons inside the gate electrode. More recent Monte Carlo simulations confirm the interplay between an increase of disorder and a concomitant decrease of the carrier mobility in the presence of a moderate concentration of extra charges and a smoothing of the energy landscape at higher concentrations [126]. By the way, broadening of the DOS distribution by counter charges also effects the Langevin-type electron hole recombination process, as was demonstrated by Monte-Carlo simulations by van der Holst and coworkers [127].

The preceding discussion of doping effects pertain to systems with low to moderate doping levels. Under this premise charge transport tends to remain of the hopping type though the shape of the DOS may be altered by the dopant. This no longer true in the case of highly doped materials that are metallic or quasi-metallic such as PEDOT [128, 129], poly-aniline [130–132], and poly-pyrrole [133, 134]. While there are calls for new concepts, notably because highly doped systems can no longer be considered as being homogeneous [128] and because there are issues concerning a possible semiconductor–metal transition, some of the experimental results can be rationalized in terms of the variable range, i.e., a modified, hopping concept [134, 135]. This is a topic in its own right and shall, therefore, not be discussed here.

5 Charge Transport in the Strong Coupling Regime

5.1 Intra-Chain Transport at Short Time Scales

In amorphous molecular systems, even the fastest hopping process is determined by the strength of inter-molecular coupling among the adjacent transport sites. A crude measure for the jump time can be obtained from the mobility extrapolated to infinite temperatures, $\mu(T \rightarrow \infty) = \mu_0$, in a $\ln \mu$ vs T^2 plot. For this rough estimation we use Einstein's ratio $eD = \mu kT$ and assume isotropic hopping with a diffusion constant $D = \frac{1}{6} a v^2$ where $a = 1$ nm is the inter-site separation and v is the inter-hop frequency. Taking $\mu_0 = 10^{-2}$ cm^2 V^{-1} s^{-1}s as a representative value for the prefactor mobility, we obtain $v = 10^{11}$ s^{-1}, equivalent to a minimum jump time of 10 ps for iso-energetic jumps.

The situation is different for systems in which the hopping sites are extended as realized in conjugated polymers. Here, one expects a hierarchy of transport processes, i.e., there should be fast on-chain transport followed by slower inter-site transport as visualized in Fig. 21. Calculations of the effective mass of charge carriers in conjugated polymers [28] predict a charge carrier mobility as high as 1,000 cm^2 V^{-1} s^{-1}, i.e., six to nine orders of magnitude larger than measured in a conventional ToF experiment. The obvious reason for this discrepancy is related to the spatial scale over which transport is measured. It is reasonable to assume that, in principle, transport is fast as long it is not affected by intrinsic or extrinsic scattering and/or localization.

The ideal systems to test this conjecture are single-crystalline poly-diacetylenes (PDAs), notably perfect PDA chains embedded in a crystalline lattice [15]. Employing the electroreflection method, Weiser and Möller [136] analyzed the

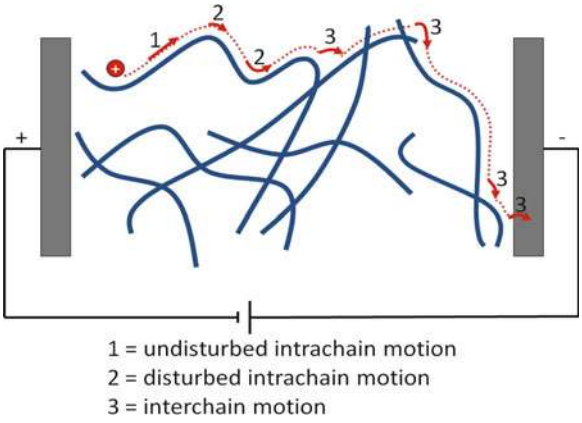

Fig. 21 A schematic view of the hierarchy of charge carrier hopping in a network of disordered conjugated polymer chains. *1* depicts ultra-fast motion within an ordered segment of the chain while *2* and *3* illustrate intra-and interchain hopping processes

reflection feature occurring approximately 0.5 eV above the excitonic absorption edge in terms of the Franz–Keldysh effect acting on the otherwise hidden valence to conduction band transition. They came up with an effective mass of approximately 0.05 m_e, in agreement with theoretical calculations [28]. This would translate into an electron mobility of approximately 1,000 $cm^2/V^{-1}s^{-1}$. So far, nobody has confirmed this prediction. Employing various methods, there is consensus that the macroscopic mobility of, presumably, electrons in crystalline PDA is greater than 1 $cm^2/V^{-1}s^{-1}$ along the chain and a factor 10^{-2} to 10^{-3} lower perpendicular to it [20, 137]. However, this value refers to macroscopic samples rather than to individual chains.

In order to obtain information pertaining to the on-chain motion, one has to rely on analogous spectroscopic studies on excitons. The Schott group studied the photoluminescence of single PDA chains in an unreacted crystalline matrix. They found that at low temperatures the excited state is an exciton that moves coherently within a distance of tens of micrometers with a coherence time of up to 1 ps. However, in a non-crystalline conjugated polymer such as MEH-PPV the phase coherence time of an optical excitation is as short as 100 fs [138, 139]. This strongly suggests that dephasing is due to scattering at static or dynamic chain imperfections rather than a generic property of conjugated polymers in general. It is straightforward to conjecture that the scattering time of charge carriers is similarly short and that their motion on macroscopic dimension is disorder controlled.

It is instructive to estimate the displacement of a charge carrier after generation. Using Einstein ratio $eD = \mu kT$, one arrives at a mean square displacement of a charge carrier, $\sqrt{\langle \Delta x^2 \rangle}$, of 20 nm (60 nm) if scattering occurred at 100 fs (1 ps) after excitation and if the initial mobility were 1,000 $cm^2/V^{-1}s^{-1}$ (Fig. 22). This has to be compared to the electronic correlation length of a chain, the so-called effective conjugation length. Usually, although not well founded, it is inferred from the dependence of the energy of a singlet excitation as a function of the lengths of oligomers. A conservative estimate is a value less than 10 nm. This indicates that

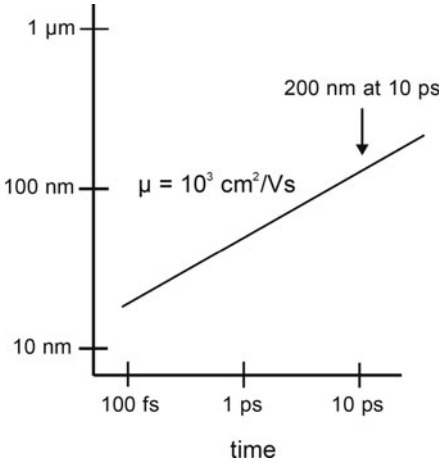

Fig. 22 A schematic plot of the mean square root displacement $\sqrt{\langle x^2 \rangle}$ of a charge carrier as a function of time for mobilities of 10^3 cm^2/Vs

one has to probe charge carrier motion on a very short length and on an ultra-fast time scale in order to be able to monitor the intrinsic, i.e., defect-free mobility.

Pioneering work on the time-resolved probing of charge carrier motion along the chain of a conjugated polymer has been performed by the Delft group employing the time resolved microwave conductivity (TRMC) technique [140]. It is an electrode-less technique. Charge carriers are generated homogeneously inside the sample by irradiation with 5–20 ns pulses of 3 MeV electrons from a van der Graaff electron accelerator. One probes their oscillatory motion by a microwave field on a short length scale yet within a nanosecond to microsecond time scale, i.e., long compared to the inverse probing microwave frequency. Typical frequencies are either 10 GHz or 34 GHz. The peak amplitude of the microwave field is of the order of 100 V/cm, i.e., low as compared to the field strengths commonly used in ToF experiments. The radiation induced conductivity is inferred from the decrease of the microwave power reflected from the cell. It is given by the product of the charge carrier concentration and their mobility. The charge concentration can be estimated from the irradiation dose and the known ionization efficiency. In order to probe charge motion on isolated polymer chains, the polymer is dissolved in benzene solution. However, the technique can also be used to study solid state effects in bulk samples. The high energy electrons absorbed inside the sample scatter on the solvent molecules and produce a virtually uniform distribution of excess electrons and benzene cations with a known concentration. Benzene cations diffuse towards the polymer chains and form polymer cations. As this diffusion-controlled reaction proceeds, an increase of the transient conductivity is observed on a time scale of hundreds of nanoseconds. This increase indicates that the positive charge on the chains are more mobile than the benzene cation in solution whose mobility is 1.2×10^{-3} $cm^2/V^{-1}s^{-1}$ at room temperature. Monitoring the motion of electrons on the polymer chain requires thorough degassing and doping with a strong hole scavenger such as tetramethyl-*p*-phenylenediamine (TMPD). In order to study selectively the motion of holes the solution can be saturated by oxygen that is an efficient scavenger for excess electrons.

A representative example for the information extracted from a TRMC experiment is the work of Prins et al. [141] on the electron and hole dynamics on isolated chains of solution-processable poly(thienylenevinylene) (PTV) derivatives in dilute solution. The mobility of both electrons and holes as well as the kinetics of their bimolecular recombination have been monitored by a 34-GHz microwave field. It was found that at room temperature both electrons and holes have high intra-chain mobilities of $\mu_- = 0.23 \pm 0.04$ $cm^2/V^{-1}s^{-1}$ and $\mu_+ = 0.38 \pm 0.02$ $cm^2/V^{-1}s^{-1}$. The electrons become trapped at defects or impurities within 4 μs while no trapping was observed for holes. The essential results are (1) that the trap-free mobilities of electrons and holes are comparable and (2) that the intra-chain hole mobility in PTV is about three orders of magnitude larger than the macroscopic hole mobility measured in PTV devices [142]. This proves that the mobilities inferred from ToF and FET experiments are limited by inter-chain hopping, in addition to possible trapping events. It also confirms the notion that there is no reason why electron and hole mobilities should be principally different. The fact

that electron mobilities observed in devices are usually much lower than the hole mobilities is exclusively due to trapping. Note that in a polymer with high lying HOMO, the LUMO level is also high, implying that inadvertent impurities such as oxidation products can act as electron traps. Analogous reasoning applies to holes. Similar experiments were performed to measure the mobility of holes along isolated chains of polyphenylenevinylene and polythiophene backbones. The values are 0.43 $cm^2/V^{-1}s^{-1}$ for MEH-PPV and 0.02 $cm^2/V^{-1}s^{-1}$ for P3HT [143].

The TRMC technique has also been applied to solid samples. It delineates the effects of sample morphology. Among the materials investigated were crystalline poly-diacetylenes, $\pi-\pi$ stacked columnar discotic liquid crystals, and conjugated polymers [144]. The largest values, on the order of 10 $cm^2/V^{-1}s^{-1}$, were found for single-crystal poly-diacetylenes. Much lower values covering the range from 0.009 to 0.125 $cm^2/V^{-1}s^{-1}$ were obtained for solution synthesized conjugated polymers with six different backbone structures. This is attributed mainly to their complex morphology and the resulting static disorder in the backbone structure. The highest mobilities for this class of materials, ca. 0.1 $cm^2/V^{-1}s^{-1}$, were found for liquid crystalline derivatives of polyfluorene and poly(phenylenevinylene). Even larger values, close to 1 $cm^2/V^{-1}s^{-1}$, were measured with discotic materials in crystalline and liquid crystalline phases. This is a signature of their self-organizing nature and hence their degree of structural order, which compensates for the weaker electronic coupling between monomeric units in the discotics as compared with covalently bonded conjugated polymers [145].

The TRMC technique has successfully been used to answer open questions regarding the relation between morphology and charge carrier mobility in layers of P3HT with different molecular weight [146]. In agreement with intuition, the TRMC experiment probes the local mobility within ordered grains in which the chains are fully elongated. It depends only weakly on molecular weight. In contrast, the macroscopic mobility of medium molecular weight layers is two orders of magnitude lower than the local mobility and *decreases* with increasing temperature. The rate limiting process is transport through disordered material surrounding ordered grains [147]. A clue for the unusual temperature dependence is provided by temperature dependent UV–Vis absorption spectra. They suggest that the aggregates undergo a "premelting" significantly below the actual melting temperature. As a result, the aggregate width decreases. The concomitant increase in width of the interlamellar zones, as well as the likely increase of disorder in these amorphous regions, is presumably the main reason for the drop in the macroscopic mobility of short chain deuterated P3HT upon heating. In contrast, long chains may interconnect the crystalline domains in high molecular weight deuterated P3HT, thus bypassing the disordered interlamellar regions and rendering the macroscopic charge transport in this material less susceptible to changes of the sample heterogeneity.

Although the above mobilities in isolated chains of conjugated polymers and in solid phases are much larger than values inferred from ToF experiments, in no case do they come close to the value of 1,000 $cm^2/V^{-1}s^{-1}$ expected for a perfect one-dimensional π-bonded polymer chain. Moreover, they are morphology-sensitive.

Improved ordering enhances the mobility. It is straightforward to conjecture that even the on-chain mobility is limited by static and dynamic disorder. A simple estimate will illustrate this. Suppose that an initially generated charge carrier had an ultra-high mobility of 1,000 $cm^2/V^{-1}s^{-1}$ and, accordingly, a diffusion coefficient of 25 cm^2/s at 295 K. Within 10 ps, which is the characteristic time scale of the microwave field, the diffusional spread of a packet of charge carriers should be 200 nm. This value is much larger that the effective conjugation length of conjugated polymers except for polydiactylenes in crystalline matrix. Therefore the carrier transport is mediated by scattering events and even blockades due to chain defects and chain ends. This notion is experimentally verified by probing the carrier motion at different microwave frequencies. If the frequency is increased their motion is confined to a smaller length scale, i.e., a carrier experiences fewer stopping events between the energy barriers. This, in turn, leads to a higher mobility upon increasing frequency. Obviously the TRMC technique does not yield a well-defined mobility value but depends on the experimental conditions. This is an inherent feature of the technique and can be exploited to extract information regarding carrier motion inside of a polymer chain. i.e., the scattering mechanism. One can even extrapolate on the carrier motion prior to scattering and blocking at a chain defect/end.

To extract pertinent information from experimental results requires a theoretical model. Based upon earlier work by Grozema et al. [143], Prins et al. [148] developed a framework to understand the effects that static disorder as well as chain dynamics have on the charge motion inside a π-conjugated chain. The basic idea is that, in conjugated oligomers and polymers, torsions, static conjugation breaks, or chain ends can all act as barriers to charge transport. The presence of these barriers leads to an increase of the charge carrier mobility with increasing microwave frequency because at higher frequency the carrier motion is probed on a smaller length scale, i.e., between these barriers. A major source of time-dependent disorder is presented by thermally driven torsional motion between repeat units of, say, a poly-phenylenevinylene or a poly-thiophene chain. It results in a variation of the electronic coupling between the repeat units. In the theory the electronic coupling was calculated by density functional theory. The results confirm that the carrier mobility probed by the TRMC technique increases with increasing length of the chain and with conjugation length. Experiments on PV oligomers with varying length and polymers containing a variable fraction of chemical conjugation breaks are in good agreement with theory. The concept of time-dependent disorder also explains why the hole mobility in MEH-PPV probed by 34-GHz radiation is 0.46 $cm^2/V^{-1}s^{-1}$ while it is only 0.02 $cm^2/V^{-1}s^{-1}$ in P3HT. The reason is the larger deviation of coplanar alignment of the structural units of P3TH as compared to MEH-PPV.

It was straightforward to apply the TRMC technique to study on-chain charge transport to ladder-type poly-phenylene (LPPP) systems because covalent bridging between the phenylene rings planarizes the chain skeleton, eliminates ring torsions, and reduces static disorder. One can conjecture that in these systems intra-chain motion should be mostly limited by static disorder and chain ends. To confirm this

notion, Prins et al. [149] measured the complex microwave conductivity in solid samples of either phenyl- or methyl-substituted LPPP with different chain lengths, i.e., of Ph-LPPP with $\langle n \rangle = 13$, 16, 35, and of MeLPPP with $\langle n \rangle = 54$, $\langle n \rangle$ being the average number of repeat units. In such an experiment, the real part of the conductivity reflects the field-induced barrier-less in-phase drift velocity of charges undergoing conventional Gaussian diffusion along an ordered, infinitely long polymer chain while the imaginary part reflects the carrier motion hindered by barriers such as chain ends. The observation that the mobility extracted from the imaginary part of the conductivity increases from 0.056 to 0.08 $cm^2/V^{-1}s^{-1}$ and to 0.14 $cm^2/V^{-1}s^{-1}$ when $\langle n \rangle$ increases from 13 to 16 and to 35 proves that the carrier motion is limited by chain ends. In order to obtain the mobility in an infinitely long chain the authors developed a model for one-dimensional diffusional motion between infinitely high reflection barriers as a function of the chain length. By extrapolation, the authors arrived at an infinite chain mobility of 30 $cm^2/V^{-1}s^{-1}$. Analogous experiments and analyzing procedures on MeLPPP in dilute solution yield a spectacular value of 600 $cm^2/V^{-1}s^{-1}$, comparable to the hypothetical value for a perfect chain [150]. The fact that the infinite chain mobility in solid LPPP-type systems is a factor of 30 less than in solution testifies to the role of interchain disorder in bulk systems. Although these extrapolated infinite-chain mobilities should be viewed with some caution, they provide an idea of how charge carriers move between scattering barriers in a conjugated polymer in a device.

When interpreting the results derived from TRMC experiments one should keep in mind that a GHz microwave field interrogates the charge carrier dynamics on a time scale ranging from nano- to microseconds. This implies that one does not probe nascent charge carriers but, rather, carriers that have had enough time to relax to energetically more favorable sections of a polymer chain. To reveal the carrier dynamics on an ultra-fast time scale requires all-optical probing. The technique of choice is time resolved terahertz (THz) spectroscopy that offers picosecond time resolution and low probing fields (kV/cm) [151–153]. It yields the far-infrared conductivity of charges generated by femtosecond light pulses. One can monitor the evolution of charge motion as a function of delay time between generation and probe pulses. The price to pay for shifting the observation window to picosecond and to sub-picosecond time scales is (1) the difficulty to retrieve the pertinent information from the raw data and (2) that the measured property is a conductivity, i.e., the product of the carrier yield and their mobility. The Sundström group [153] applied this technique to study holes on low-bandgap conjugated polymers consisting of an alternating sequence of a low bandgap unit as an electron accepting group and a dialkoxy-phenylene unit. The copolymer was blended with the fullerene derivative PCBM which is often used as an acceptor in organic solar cells. Upon photoexcitation the electron is transferred to the PCBM. The hole remains on the polymer chain and is responsible for the ultra-fast conductivity because the electron motion among the PCBM units is much slower. From the intricate analysis of the experimental results combined with simulation the authors conclude an intrinsic carrier mobility of 40 $cm^2/V^{-1}s^{-1}$ within unperturbed chain segments comprising about four repeat units. Like the electron, the hole generated by the

dissociation process carries an initial excess of kinetic energy that allows it to pass easily over potential barriers with an intrinsic mobility of about 2 $cm^2/V^{-1}s^{-1}$. Subsequently, the hole cools down at an initial relaxation rate of 1/180 fs^{-1} and gets trapped at an initial rate of 1/860 fs^{-1}. This is manifested by a steep drop of the conductivity. The results are consistent with the notion of an ultra-fast mobility of charges on a π-conjugated chain between scattering events. They also indicate that the time averaged mobility derived from a TRMC experiment is that of charge carriers that already suffered some relaxation.

An independent and complementary method to measure the charge carrier mobility on ultra-fast time scales has recently been introduced by Devizis et al. [154]. It is based on time resolved electric field induced second harmonic generation (SHG). This method is commonly used to determine molecular hyperpolarizabilities. Any process that changes the electric field distribution in the material will affect the temporal SHG signal. In turn, the SHG intensity can be taken as a probe of changes of the electric field due to charge motion. Upon generating charge carriers in a charged capacitor by a short laser flash the moving charge partially shields the electric field and the SHG efficiency decreases. Measuring the decrease of the SHG signal as a function of time after the laser pulse yields the time dependence of the carrier motion up to a detection time of 3 ns. Integrated photocurrents measured within a time window of 10 ns to 10 μs complement the information on the time dependence of the mobility. The technique was applied to poly-spiro-bifluorene-*co*-benzothiadiazol (PSF-BT). It turns out that the sum of the electron and hole mobilities probed at 1 ps after excitation is about 0.1 $cm^2/V^{-1}s^{-1}$. It decreases to 10^{-6} $cm^2/V^{-1}s^{-1}$ at 1 μs featuring an $\ln \mu$ vs $t^{-\beta}$ law with β ranging from 0.84 at lower fields (about 4×10^5 V/cm) to 0.75 (at about 1.5×10^6 V/cm) (see Fig. 23). These results prove unambiguously that within a time range of 6 decades transport is dispersive and, concomitantly, controlled by disorder.

5.2 *Band Transport*

In this chapter we so far focussed on charge transport in organic solids that are used as active materials in modern opto-electronic devices such as OLEDs, solar cells, field effect transistors, and photocopiers. Dictated by the need for cost-efficient device manufacturing and the realization of optimized structure-property relations for special applications, the active device elements are usually non-crystalline, if not amorphous. This implies that charge transport is of the hopping type. It turned out, though, that crystalline organic semiconductors may profitably be employed as active layers in field effect transistors where band-like carrier transport prevails. For this reason we shall very briefly address recent developments in this area without attempting to cover the growing field of organic field effect transistors in greater detail.

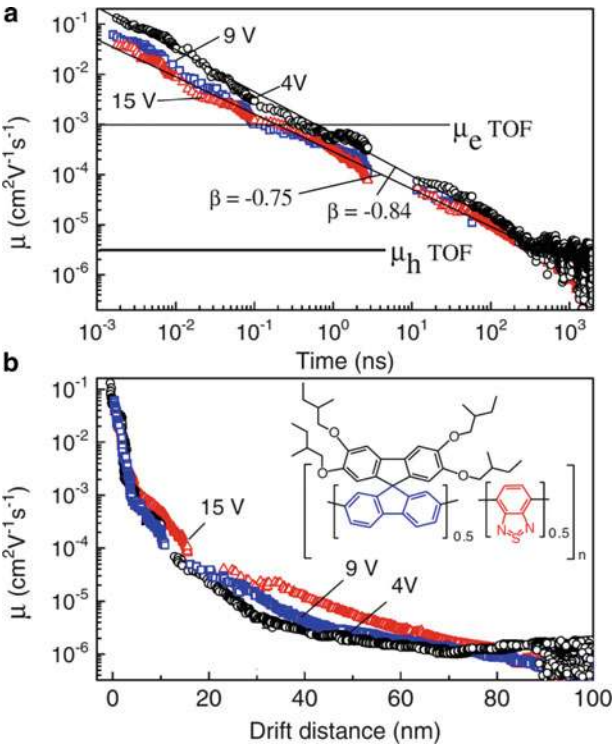

Fig. 23 (**a**) Dependence of the hole mobility in a film of poly-spiro-bifluorene-*co*-benzothiazole (PSF-BT) as function of the time elapsed after charge carrier generation by a 130 fs laser pulse at different applied voltages. The *horizontal lines* represent the electron and hole mobilities inferred from ToF experiments. (**b**) Momentary mobility as a function of the averaged distance that a carrier travelled after a given time. The *inset* depicts the chemical structure of PSF-BT. From [154] with permission. Copyright (2009) by the American Institute of Physics

Band-like charge transport in molecular crystals was investigated experimentally in the 1980s and 1990s. The pioneering work of Karl and his group in Stuttgart showed that close to and below room temperature, and dependent on crystallographic direction, the mobility of both electrons and holes feature a T^{-n} law with $n = 2$–3, provided that they can be purified efficiently (see [155]). For less pure crystals, the mobility is temperature activated with an activation energy that is given by the difference of the HOMO (LUMO) levels between host and guest. This proves that transport is trap limited. The temperature at which the transition from band to trap limited transport occurs depends on the trap concentration and the trap depth. In view of the narrow width of valence and conduction bands in molecular crystals the charge carrier mean free paths are only a few lattice sites at most. This implies that transport is on the borderline between being coherent and incoherent. This problem has been discussed intensively in the books of Pope and Swenberg [45] and of Silinsh and Capek [156] and recently

by Fratini and Chiuchi [157]. A comprehensive review of more recent advances has been published by Coropceanu et al. [10]. Based upon quantum chemical treatments the authors developed a consistent theoretical framework of the electronic coupling and the electron–phonon interaction as a function of the lattice structure. The electronic transfer integral is the matrix element that couples the wavefunctions of two charge-localized states via an electronic Hamiltonian of the system. It depends on the mutual orientation of the molecules and thus on the crystallographic direction. Typical values range between about 10 and 83 meV for the (100) direction of a rubrene crystal. Since the widths of the transport bands is four times the transfer integral, this results in bandwidths of the order of some 10–100 meV. Although these calculations refer to molecular crystals they are also relevant for disorder systems because the charge carrier mobility extrapolated to infinite temperature (μ_0) depends on the electronic coupling among the structural building blocks.

Organic crystalline materials that may be used in FETs are rubrene and pentacene because the relevant electronic transfer integrals are comparatively large. Accordingly, both materials have comparatively high hole mobilities of 10 $cm^2/V^{-1}s^{-1}$ or higher at room temperature if measured in FET configuration (see [158]). Podzorov et al. [159] measured a value of 30 $cm^2/V^{-1}s^{-1}$ at 200 K. In later work Zeis et al. [160] reported a maximal mobility of 13 $cm^2/V^{-1}s^{-1}$ with strong anisotropy. A decrease of μ at lower temperatures is a signature of charge carrier trapping. Applying a hot wall deposition method, a hole mobility of only 2.4 $cm^2/V^{-1}s^{-1}$ in rubrene has been measured. Obviously sample preparation and purification have a profound effect on the crystal properties, particularly if the sample is polycrystalline instead of single crystalline [161]. For pentacene, an extrapolated value as high as 50 $cm^2/V^{-1}s^{-1}$ for the in-plane mobility has been inferred from space-charge-limited current measurements performed in surface configuration [162]. A high hole mobility is consistent with a valence bandwidth along the 100 direction of 240 meV at 120 K and 190 meV at 295 K determined from photoemission spectroscopy [163] and with DFT calculations for the charge transfer integral that yield values of 70–75 meV [10]. However, the way the sample is prepared has a major effect on the mobility. This is illustrated by the work of Minarin et al. [164]. These authors measured the hole mobility in a single-grain pentacene FET within a temperature range between 300 K and 5.8 K and found a room temperature mobility of about 1 $cm^2/V^{-1}s^{-1}$ and weakly activated transport below with an activation energy of 4.6 meV. In a polycrystalline sample the room temperature mobility is about 0.3 $cm^2/V^{-1}s^{-1}$ and the activation energy is 55 meV. Obviously, grain boundaries act as charge carrier traps [165, 166].

In an attempt to combine band-like charge carrier motion realized in an – inevitably fragile – crystalline FET structure with structural robustness and flexibility, Sakanoue and Sirringhaus [167] prepared FETs using spin coated films of 6,13-bis(triisopropylsilylethynyl)(TIPS)-pentacene films in contact with a perfluorinated, low dielectric-constant polymer gate electrode. The (linear) hole mobility at room temperature is 0.8 $cm^2/V^{-1}s^{-1}$ with tendency of an apparent "band-like" negative temperature coefficient of the mobility ($d\mu/dT < 0$).

The authors use optical spectroscopy of gate-induced charge carriers to show that, at low temperature and small lateral electric field, charges become localized onto individual molecules in shallow trap states, but that at moderate temperatures an electric field is able to detrap them, resulting in transport that is not temperature-activated. This work demonstrates that transport in such systems can be interpreted in terms of classical semiconductor physics and there is no need to invoke one-dimensional Luttinger liquid physics [168].

6 Charge Injection

6.1 Mechanism of Charge Carrier Injection

In most cases, injection from the electrodes is the process by which charge carriers are generated in OLEDs and FETs. Usually it is limited by an energy barrier between the Fermi-level of the electrode and the transport levels of the dielectric. In conventional crystalline inorganic semiconductors, the relevant processes are either Richardson–Schottky emission or Fowler–Nordheim tunneling (see Fig. 24). The former process implies that a thermally excited electron from the Fermi level travels across the maximum of the electrostatic potential modified by the coulomb potential of the image charge and the applied electric field without being scattered. It gives rise to an Arrhenius-type of temperature dependence ($\ln j \propto T$), and a Poole–Frenkel-type of field dependence, i.e., $\ln j \propto \sqrt{F}$. In the classic Fowler–Nordheim case, one ignores the image potential and one assumes that an electron at the Fermi level of the metal tunnels through a triangular potential barrier set by the interfacial energy barrier and the applied potential. For both mechanisms, the crucial condition is that there is strong electronic coupling among the constituting lattice elements that leads to wide valence and conduction bands. This implies that the scattering length of charge carriers is much larger than the interatomic separation. In organic solids this condition is violated because electronic coupling between molecules is of van der Waals type and thus weak. Accordingly, transport is incoherent and of the hopping type. Therefore, the condition of collision-free charge injection across the maximum of the electrostatic potential, implied by Schottky theory, is violated. An experimental signature of this failure of the classic injection models is that the temperature dependence of the injection current is (1) weaker than expected based upon the estimated energy barriers and (2) sub-linear on an Arrhenius scale. This excludes a classic Richardson–Schottky emission process, yet this also eliminates Fowler–Nordheim tunneling as a mechanism since these observations hold even within a field range at which tunneling has got to be inefficient. Thus, theoretical reasoning and experimental observation imply that the classical inorganic semiconductor mechanisms for charge injection do not apply. Therefore, alternative, more suited approaches are needed.

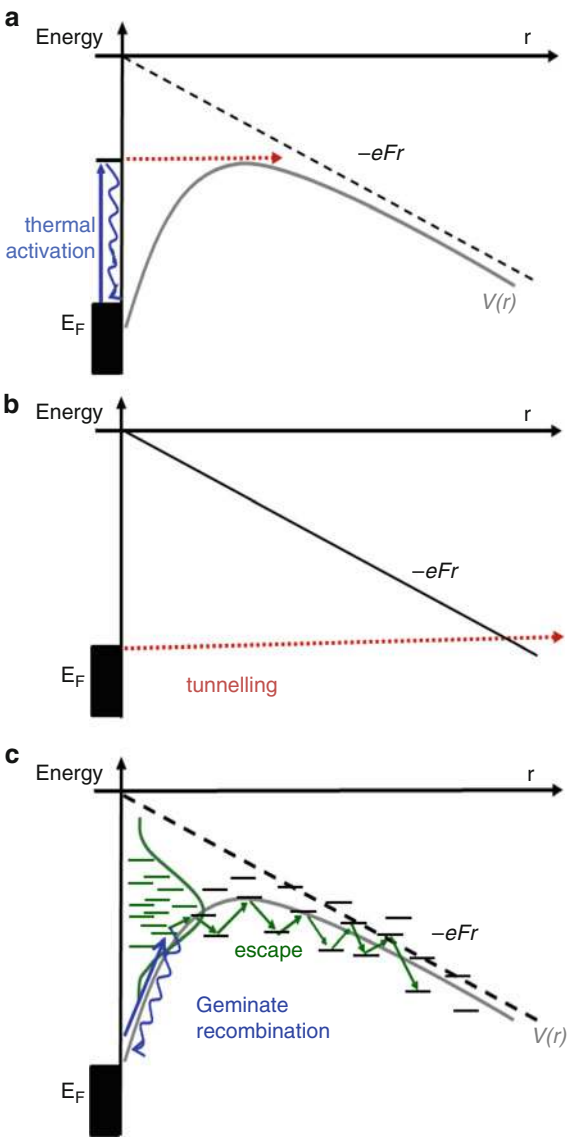

Fig. 24 Schematic representation of electron injection from a metallic electrode into a semiconductor (**a**) via Schottky emission, (**b**) via Fowler–Nordheim tunneling, and (**c**) via hopping in a disordered organic solid. F is the applied electric field, r denotes the distance from the electrode

Based upon simulation [169] and analytical theory [170] a model has meanwhile been developed that takes into account (1) the existence of the image charge at the electrode, (2) the hopping-type of charge transport, and (3) the presence of disorder existing in a non-crystalline system. The underlying idea, originally introduced by Gartstein and Conwell [171], is that a thermally activated jump raises an electron from the Fermi level of the electrode to a tail state of the density of states distribution of transport sites of the dielectric medium subject to the condition

that this site has at least one hopping neighbor at equal or even lower energy. It is fulfilled by optimizing a transport parameter with regard to both jump distance and jump energy. This condition ensures that the primarily injected carrier can continue its motion away from the interface rather than recombine with its image charge in the electrode. Subsequently, the carrier is considered to execute a diffusive random walk in the combined coulomb potential of the image charge and the externally applied potential, and this is described by using a one-dimensional Onsager's theory. Simulation and analytical theory for injection barriers ranging from 0.2 to 0.7 eV and for temperatures between 300 and 200 K are mutually consistent. Apparently, the neglect of the stochastic nature of the carrier motion in the vicinity of the electrode as well as the neglect of disorder on the one-dimensional Onsager-type escape process is uncritical in the considered parameter regime. The field dependence of the injection efficiency follows a Poole–Frenkel-type law and bears out a sub-linear temperature dependence on an Arrhenius scale with a mean activation energy that is significantly lower than one might suspect based upon the literature values of the work-function of the electrode and the electron affinity/ionization energy of the dielectric. The qualitative explanation of this ubiquitously observed phenomenon [172] is the following. Upon lowering the temperature, the transport energy, and therefore also the critical site energy from which a charge carrier can start its diffusive motion within the DOS distribution, decreases. Consequently the activation energy needed for injection is not constant but decreases with decreasing temperature.

A textbook example for the successful application of the model of Arkhipov et al. is the work of van Woudenbergh et al. [173]. More recently, Agrawal et al. [106] compared injection limited currents and space-charge-limited currents in a copper-phthalocyanine sandwich cell with ITO and Al electrodes. An analysis of experimental data yields consistent values for the width of the DOS distribution as well as for inter-site separation [174]. These studies support the model of thermally activated injection into a Gaussian DOS distribution of hopping sites and confirm the notion that disorder facilitates injection because it lowers the injection barrier, although the transport velocity decreases with increasing disorder.

In 2000, A. Burin and M. Ratner [175] presented an injection model based upon the idea that injection and transport occur through one-dimensional straight paths, effectively lowering the injection barrier. Meanwhile, van der Holst et al. [127] developed a three-dimensional master equation model that includes the disorder in the transport and avoids the shortcomings of the one-dimensional model, in which carrier blockade events can be crucial (Fig. 25). It is fair to say, though, that for devices operating close to room temperature, the simpler treatment of Arkhipov et al. is sufficient. It is worth pointing out, however, that all these treatments rely on the notion that the initial injection event is largely controlled by the existence of tail states of the DOS at the interface and that it is defined by an energy vs hopping range optimization procedure. Since in a bulk system the low energy sites are spatially fixed, the injection process is NOT spatially homogeneous, but filamentary as pointed out by van der Holst et al.

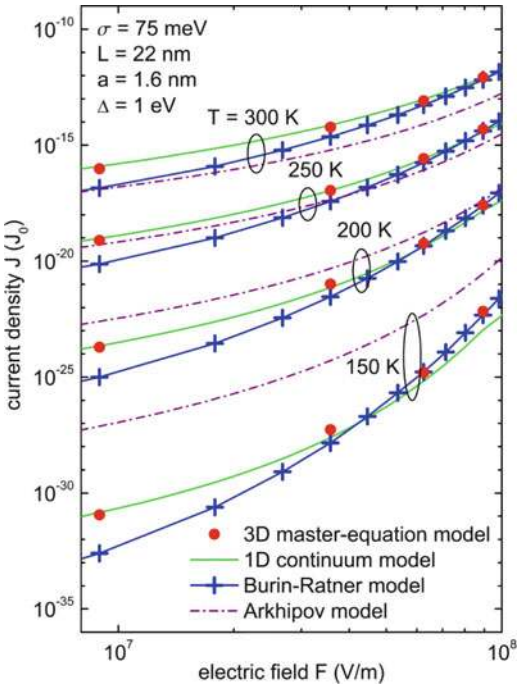

Fig. 25 Comparison of the predictions of various models for current injection from a metal electrode into a hopping system featuring a Gaussian DOS of variance $\sigma = 75$ meV as a function of the electric field at different temperatures. The 1D continuum and the 3D master equation model have been developed by van der Holst et al. [127]. The calculations based upon the Burin-Ratner and the Arkhipov et al. models are taken from [175] and [170] respectively. Parameters are the sample length L, the intersite separation a and the injection barrierΔ. From [127] with permission. Copyright (2009) by the American Institute of Physics

The magnitude of the injection barrier is open to conjecture. Meanwhile there is consensus that energy barriers can deviate significantly from the values estimated from vacuum values of the work-function of the electrode and from the center of the hole and electron transporting states, respectively. The reason is related to the possible formation of interfacial dipole layers that are specific for the kind of material. Photoelectron spectroscopy indicates that injection barriers can differ by more than 1 eV from values that assume vacuum level alignment [176, 177]. Photoemission studies can also delineate band bending close to the interface [178].

An example of the difficulties encountered when trying to fabricate an ohmic electrode, able to sustain a space-charge-limited current, is the recent work of the Neher group [179]. The authors deposited barium as an electron injection cathode on top of an electron transporting polymer based on a naphthalene diimide core whose LUMO is as low as −4 eV below vacuum level. Although the Fermi level of barium should be above the LUMO of the polymer, the electron current is,

unexpectedly, contact-limited rather than space-charge-limited. It appears that evaporation of reactive metals onto layers of conjugated polymers introduces injection barriers through the formation of oxides and chemical defects. While this effect can be masked by the low bulk currents in the majority of n-type polymers with low electron mobilities, it is important in the case of this naphthalene diimide polymer that has an unusually high electron mobility of 3.5×10^{-3} $cm^2/V^{-1}s^{-1}$ at 295 K.

6.2 Ohmic Injection

At low injection barriers the surface charge injected into a layer next to the electrode can become comparable with the capacitor charge. If this condition is met at arbitrary applied voltage, such a contact serves as an "ohmic" electrode from which charge injection occurs. In this case the current is solely determined by transport within the bulk of the dielectric rather than by the injection process, i.e., by the charge carrier mobility, and it is considered to be space-charge-limited (SCL). Establishment of this condition depends on both the magnitude of the injection barrier and the charge carrier mobility. For typical OLED parameters, the critical energy barrier is about 0.3 eV [180, 181]. Interfacial doping, for instance by electron acceptors such as C_{60} [182, 183] and the more electronegative tetrafluoronocyanoquinodimethane (F_4-TCNQ) [184], can lower the injection barrier. Another way to improve injection is to insert a thin interfacial layer, such as a self-assembled monolayer [185]. The effect of such a layer can be due to interfacial tunneling [186] or to changes of the sample morphology and/or the electronic structure at the interface.

It is obvious that in an OLED efficient charge injection is crucial. A simple estimate will illustrate this. Suppose that a concentration n of charge carriers equivalent to the capacitor charge CV, where C is the capacitance per unit area and V is the applied voltage, is distributed homogeneously within a dielectric layer of thickness d. We find $n = \dfrac{\varepsilon\varepsilon_0 F}{ed}$. The bimolecular recombination time with a counter charge is $\frac{1}{n\gamma}$, where γ is the bimolecular recombination coefficient. Chemical kinetics predicts $\gamma = 4\pi\langle R\rangle(D_+ + D_-)$, where $\langle R\rangle$ is the mean distance at which charges recombine, and D_+ and D_- are the diffusion constants of the charge carriers. It is taken to be the coulomb capture radius $\langle R\rangle = \frac{e^2}{4\pi\varepsilon_0\varepsilon\, kT}$. Using the Einstein ratio $eD = \mu kT$ between the sum of the diffusion coefficients D and the sum of the mobilities μ, one obtains $\frac{1}{n\gamma} = \frac{d}{\mu F}$, i.e., $\frac{1}{n\gamma}$ is equal to the transit time of the charge carrier. This shows that in an OLED the concentration of positive and negative charges must at least be comparable to the capacitor charge in order to ensure that charges recombine bimolecularly rather than wastefully at the electrodes. A crucial test of this condition is to check whether or not the unipolar current injected from a supposedly ohmic electrode obeys Childs's law for SCL

current flow, $j = \frac{9}{8}\varepsilon\,\varepsilon_0\mu\frac{F^2}{d}$, i.e., at a given electric field the current must follow a 1/d dependence on sample thickness [106]. There should also be consistency regarding the value of the mobility inferred from a ToF experiment performed under weak injection conditions and the SCL current [187]. However, even if one would expect an electrode to be ohmic based upon the estimate for the injection barrier, ohmicity is not always granted. An example is the work on poly(9, 9′-dioctyl-fluorenyl-2,7-diyl)-*co*-(4,4′-N-(4-*sec*-butyl))diphenylamine (TBB) with ITO/PEDOT:PSS serving as a hole injecting electrode. Due to appropriate synthesis and purification procedures, the mobility can be raised to 10^{-2} $cm^2/V^{-1}s^{-1}$. Unexpectedly, the hole current is not space-charge-limited, most likely because the sheet resistance of the ITO/PEDOT:PSS electrode can become the limiting parameter relative to the bulk resistance if the mobility is high [188]. Obviously the design of an ohmic electrode with low sheet resistance, able to sustain a large SCL current, is still a challenge.

7 Summary and Conclusions

In this chapter we have tried to summarize the current understanding of charge transport in organic semiconductors. It includes a brief description of the methods to measure charge transport, an overview of pertinent experimental results, and an outline of theoretical concepts. These conceptual frameworks had been developed in the course of a most fruitful interaction between theoreticians and experimentalists. This scientific progress can also be expected to bring about technological advances. For example, in the beginning of electrophotography it was not at all clear whether or not an organic material like a polymer could ever replace inorganic photoreceptors such as selenium and arsenic selenide due to the omnipresent charge carrier trapping in the organic material. Polymers can never be purified up to the level attained in silicon or selenium. However, it was the intuition of organic chemists and electrochemists who realized that one can overcome the problem of charge carrier trapping in an organic photoreceptor used in xerography by using a transport material with low oxidation potential, so that most impurities are inactive. Nowadays, photocopying machines with organic semiconductors are present in virtually every office worldwide.

In a similar way, the role of disorder, that inevitably is present in a polymer or a molecularly doped polymer, can now be quantified due to the significant advances in our theoretical understanding that have been outlined in this chapter. Ultimately, this will allow for the design of transport materials with sufficiently large carrier mobilities. Until we arrive there, however, it is worth recalling what we do understand and which challenges remain. Today, we have a reasonably well-founded understanding of the macroscopic, i.e., ensemble-averaged process of charge transport in disordered organic solids. This applies to single-component

materials as well as to multi-component materials such as doped organic semiconductors. The corresponding models were presented in Sects. 3 and 4. However, our understanding on the microscopic scale, in particular on very short time scales and over very short distances, is still incomplete. The present advances towards understanding this regime have been outlined in Sect. 5. These short-scale, short-range processes are of particular importance to solar cells.

It is a generally accepted notion that the most efficient organic cells utilize donor-acceptor blends forming internal heterojunctions as active materials. In these cells the primary step is the absorption of a photon in (usually) the donor phase. The generated exciton diffuses towards the internal interface and transfers an electron to the acceptor, thus forming an electron-hole pair (synonymously called a charge transfer (CT) state or geminate pair). The pair has to dissociate and both electron and hole must drift under the action of the built-in potential and be collected at the electrodes without suffering further geminate and non-geminate recombination. Meanwhile there is consensus that the crucial step is the escape of the electron-hole pair from its mutual coulomb potential. It is an open question, though, why in efficient organic cells the geminate recombination of the initially generated pair is greatly reduced. (1) Is there a disorder related blockade of the non-radiative decay of the pair [61], (2) is the formation of the geminate pair an ultra-fast process during which the carriers move in a high mobility state (see Sect. 5) so that the initially generated pair is only loosely bound, (3) is there a shielding of the coulomb potential due to dark dipoles existing at their internal interface [189], (4) is the dissociation process disorder assisted [190–192], and (5) does the conjugation length of the donor or acceptor play a role [193]? At the moment there are no unique answers to these questions and there is likely to continue to be no unique answers because polymers and small molecule devices should behave differently. It is highly probable, however, that microscopic charge transport, controlled by morphology, plays a crucial role, and current research points this way [194–197].

The progress reported here has been achieved through simultaneous advances in theoretical methodology and experimental techniques and, importantly, through good scientific communication between theoretically and experimentally-minded physicists and chemists. Our experimental abilities as well as computing powers and theoretical methodologies are constantly expanding. Optical experiments can be conducted in the femtosecond range, techniques such as the use of terahertz spectroscopy allow for the probing of carrier mobility at ultrafast time scales, and sophisticated computer simulations can be based on realistic models of the organic film morphology. It will be interesting to see which concepts will have been established in the future concerning charge transport on short time scales and distances, and to which advanced optoelectronic applications our established knowledge on macroscopic carrier transport has led us from its simple beginnings in the photocopying process.

References

1. Borsenberger PM, Weiss DS (1998) Organic photoreceptors for xerography. Marcel Dekker, New York
2. Friend RH, Gymer RW, Holmes AB, Burroughes JH, Marks RN, Taliani C, Bradley DDC, Dos Santos DA, Bredas JL, Logdlund M, Salaneck WR (1999) Electroluminescence in conjugated polymers. Nature 397:121
3. Forrest SR (2004) The path to ubiquitous and low-cost organic electronic appliances on plastic. Nature 428:911
4. All Articles in (2007) Special issue on organic electronics and optoelectronics. Chem Rev 107:923
5. Müllen K, Scherf U (2006) Organic light emitting devices: synthesis, properties and applications. Wiley-VCH, Weinheim
6. Yersin H (2007) Highly efficient OLEDs with phosphorescent materials. Wiley-VCH, Weinheim
7. Hertel D, Bässler H (2008) Photoconduction in amorphous organic solids. Chemphyschem 9:666
8. Chang EK, Rohlfing M, Louie SG (2000) Excitons and optical properties of alpha-quartz. Phys Rev Lett 85:2613
9. Kador L (1991) Stochastic-theory of inhomogeneous spectroscopic line-shapes reinvestigated. J Chem Phys 95:5574
10. Coropceanu V, Cornil J, da Silva DA, Olivier Y, Silbey R, Bredas JL (2007) Charge transport in organic semiconductors. Chem Rev 107:926
11. Warta W, Stehle R, Karl N (1985) Ultrapure, high mobility organic photoconductors. Appl Phys A 36:163
12. Karl N (2000) In: Madelung O, Schulz M, Weiss H (eds) Semiconductors (Landolt-Boernstein (New Series), Group III). Springer, Heidelberg, p 106
13. Karl N (2001) In: Farchioni R, Grosso G (eds) Organic electronic materials. Springer-Verlag, Berlin
14. Schwoerer M, Wolf HC (2007) Organic molecular solids. Wiley-VCH, Weinheim
15. Schott M (2006) In: Lanzani G (ed) Photophysics of molecular materials: from single molecules to single crystals. Wiley-VCH, Weinheim, p 49
16. Collini E, Scholes RD (2009) Coherent intrachain energy migration in a conjugated polymer at room temperature. Science 323:369
17. Barford W, Trembath D (2009) Exciton localization in polymers with static disorder. Phys Rev B 80:165418
18. Hoffmann ST, Bässler H, Köhler A (2010) What determines inhomogeneous broadening of electronic transitions in conjugated polymers. J Phys Chem B 114:17037
19. Bässler H (1985) In: Bloor D, Chance RR (eds) Polydiacetylenes. Martinus Nijhof, Dordrecht, The Netherlands, p 135
20. Blum T, Bässler H (1988) Reinvestigation of generation and transport of charge-carriers in crystalline polydiacetylenes. Chem Phys 123:431
21. Su WP, Schrieffer JR, Heeger AJ (1979) Solitons in polyacetylene. Phys Rev Lett 42:1698
22. Heeger AJ, Kivelson S, Schrieffer JR, Su WP (1988) Solitons in conducting polymers. Rev Mod Phys 60:781
23. Fesser K, Bishop AR, Campbell DK (1983) Optical-absorption from polarons in a model of polyacetylene. Phys Rev B 27:4804
24. Sariciftci NS (1997) Primary photoexcitations in conjugated polymers: molecular exciton versus semiconductor band model. Word Scientific, Singapore
25. Longuet-Higgins HC, Salem L (1959) The alternation of bond lengths in long conjugated chain molecules. Proc Royal Soc London A 251:172

26. Salaneck WR, Staftström S, Bredas J-L (1996) Conjugated polymer surfaces and interfaces. Electronic and chemical structure of interfaces for polymer light emitting devices. Cambridge University Press, Cambridge
27. Weiser G (1992) Stark-effect of one-dimensional Wannier excitons in polydiacetylene single-crystals. Phys Rev B 45:14076
28. Van der Horst JW, Bobbert PA, Michels MAJ, Bässler H (2001) Calculation of excitonic properties of conjugated polymers using the Bethe–Salpeter equation. J Chem Phys 114:6950
29. Albrecht U, Bässler H (1995) Efficiency of charge recombination in organic light-emitting-diodes. Chem Phys 199:207
30. Kohler BE, Woehl JC (1995) A simple-model for conjugation lengths in long polyene chains. J Chem Phys 103:6253
31. Romanovskii YV, Gerhard A, Schweitzer B, Personov RI, Bässler H (1999) Delayed luminescence of the ladder-type methyl-poly(para-phenylene). Chem Phys 249:29
32. Monkman AP, Burrows HD, Hamblett I, Navaratnam S, Scherf U, Schmitt C (2000) The triplet state of the ladder-type methyl-poly(p-phenylene) as seen by pulse radiolysis-energy transfer. Chem Phys Lett 327:111
33. Hertel D, Setayesh S, Nothofer HG, Scherf U, Müllen K, Bässler H (2001) Phosphorescence in conjugated poly(para-phenylene)-derivatives. Adv Mater 13:65
34. Köhler A, Wilson JS, Friend RH, Al-Suti MK, Khan MS, Gerhard A, Bässler H (2002) The singlet-triplet energy gap in organic and Pt-containing phenylene ethynylene polymers and monomers. J Chem Phys 116:9457
35. Köhler A, Beljonne D (2004) The singlet-triplet exchange energy in conjugated polymers. Adv Funct Mater 14:11
36. Hertel D, Bässler H, Scherf U, Hörhold HH (1999) Charge carrier transport in conjugated polymers. J Chem Phys 110:9214
37. Deussen M, Bässler H (1993) Anion and cation absorption-spectra of conjugated oligomers and polymer. Synth Met 54:49
38. Bäuerle P, Segelbacher U, Maier A, Mehring M (1993) Electronic-structure of monomeric and dimeric cation radicals in end-capped oligothiophenes. J Am Chem Soc 115:10217
39. Nöll G, Lambert C, Lynch M, Porsch M, Daub J (2008) Electronic structure and properties of poly- and oligoazulenes. J Phys Chem C 112:2156
40. Osterholm A, Petr A, Kvarnstrm C, Ivaska A, Dunsch L (2008) The nature of the charge carriers in polyazulene as studied by in situ electron spin resonance−UV−visible−near-infrared spectroscopy. J Phys Chem B 112:14149
41. van Haare JAEH, Havinga EE, van Dongen JLJ, Janssen RAJ, Cornil J, Bredas JL (1998) Redox states of long oligothiophenes: two polarons on a single chain. Chem Eur J 4:1509
42. Kadashchuk A, Arkhipov VI, Kim C-H, Shinar J, Lee D-W, Hong Y-R, Jin J-I, Heremans P, Bässler H (2007) Localized trions in conjugated polymers. Phys Rev B 76:235205
43. Furukawa Y (1996) Electronic absorption and vibrational spectroscopies of conjugated conducting polymers. J Phys Chem 100:15644
44. Sakamoto A, Nakamura O, Tasumi M (2008) Picosecond time-resolved polarized infrared spectroscopic study of photoexcited states and their dynamics in oriented poly(p-phenylene-vinylene). J Phys Chem B 112:16437
45. Pope M, Swenberg CE (1999) Electronic processes in organic crystals and polymers. Oxford University Press, Oxford
46. Arkhipov VI, Fishchuk II, Kadashchuk A, Bässler H (2007) In: Hadziioannou G, Malliaras GG (eds) Semiconducting polymers: chemistry, physics, engineering, vol 1. Wiley-VCH, Weinheim
47. Borsenberger PM, Pautmeier L, Bässler H (1991) Hole transport in bis(4-N, N-diethylamino-2-methylphenyl)-4-methylphenylmethane. J Chem Phys 95:1258
48. Markham JPJ, Anthopoulos TD, Samuel IDW, Richards GJ, Burn PL, Im C, Bässler H (2002) Nondispersive hole transport in a spin-coated dendrimer film measured by the charge-generation-layer time-of-flight method. Appl Phys Lett 81:3266

49. Gambino S, Samuel IDW, Barcena H, Burn PL (2008) Electric field and temperature dependence of the hole mobility in a bis-fluorene cored dendrimer. Org Electron 9:220
50. Klenkler RA, Xu G, Aziz H, Popovic ZD (2006) Charge-carrier mobility in an organic semiconductor thin film measured by photoinduced electroluminescence. Appl Phys Lett 88:242101
51. Bange S, Kuksov A, Neher D (2007) Sensing electron transport in a blue-emitting copolymer by transient electroluminescence. Appl Phys Lett 91:143516
52. Juska G, Arlauskas K, Viliunas M, Kocka J (2000) Extraction current transients: new method of study of charge transport in microcrystalline silicon. Phys Rev Lett 84:4946
53. Bange S, Schubert M, Neher D (2010) Charge mobility determination by current extraction under linear increasing voltages: case of nonequilibrium charges and field-dependent mobilities. Phys Rev B 81:035209
54. Bässler H (1993) Charge transport in disordered organic photoconductors – a Monte-Carlo simulation study. Phys Status Solidi B 175:15
55. Miller A, Abrahams E (1960) Impurity conduction at low concentrations. Phys Rev 120:745
56. Arkhipov VI, Emelianova EV, Adriaenssens GJ (2001) Effective transport energy versus the energy of most probable jumps in disordered hopping systems. Phys Rev B 6412:125125
57. Pautmeier L, Richert R, Bässler H (1991) Anomalous time-independent diffusion of charge-carriers in a random potential under a bias field. Phil Mag B 63:587
58. Richert R, Pautmeier L, Bässler H (1989) Diffusion and drift of charge-carriers in a random potential – deviation from Einstein law. Phys Rev Lett 63:547
59. Roichman Y, Tessler N (2002) Generalized Einstein relation for disordered semiconductors – implications for device performance. Appl Phys Lett 80:1948
60. Tal O, Epstein I, Snir O, Roichman Y, Ganot Y, Chan CK, Kahn A, Tessler N, Rosenwaks Y (2008) Measurements of the Einstein relation in doped and undoped molecular thin films. Phys Rev B 77:201201
61. Tessler N, Preezant Y, Rappaport N, Roichman Y (2009) Charge transport in disordered organic materials and its relevance to thin-film devices: a tutorial review. Adv Mater 21:2741
62. Borsenberger PM, Pautmeier LT, Bässler H (1993) Scaling behavior of nondispersive charge-transport in disordered molecular-solids. Phys Rev B 48:3066
63. Fishchuk II, Kadashchuk A, Bässler H, Abkowitz M (2004) Low-field charge-carrier hopping transport in energetically and positionally disordered organic materials. Phys Rev B 70:245212
64. Movaghar B, Grünewald M, Ries B, Bässler H, Wurtz D (1986) Diffusion and relaxation of energy in disordered organic and inorganic materials. Phys Rev B 33:5545
65. Gartstein YN, Conwell EM (1994) High-field hopping mobility of polarons in disordered molecular-solids – a Monte-Carlo study. Chem Phys Lett 217:41
66. Dunlap DH, Parris PE, Kenkre VM (1996) Charge-dipole model for the universal field dependence of mobilities in molecularly doped polymers. Phys Rev Lett 77:542
67. Cordes H, Baranovskii SD, Kohary K, Thomas P, Yamasaki S, Hensel F, Wendorff JH (2001) One-dimensional hopping transport in disordered organic solids. I. Analytic calculations. Phys Rev B 63:094201
68. Hirao A, Nishizawa H, Sugiuchi M (1995) Diffusion and drift of charge carriers in molecularly doped polymers. Phys Rev Lett 75:1787
69. Schein LB, Glatz D, Scott JC (1990) Observation of the transition from adiabatic to nonadiabatic small polaron hopping in a molecularly doped polymer. Phys Rev Lett 65:472
70. Fishchuk II, Kadashchuk A, Bässler H, Nespurek S (2003) Nondispersive polaron transport in disordered organic solids. Phys Rev B 67:224303
71. Parris PE, Kenkre VM, Dunlap DH (2001) Nature of charge carriers in disordered molecular solids: are polarons compatible with observations? Phys Rev Lett 87:126601
72. Schein LB, Tyutnev A (2008) The contribution of energetic disorder to charge transport in molecularly doped polymers. J Phys Chem C 112:7295

73. Borsenberger PM, Bässler H (1991) Concerning the role of dipolar disorder on charge transport in molecularly doped polymers. J Chem Phys 95:5327
74. Scher H, Montroll EW (1975) Anomalous transit-time dispersion in amorphous solids. Phys Rev B 12:2455
75. Arkhipov VI, Iovu MS, Rudenko AI, Shutov SD (1979) Analysis of the dispersive charge transport in vitreous 0.55 As_2S_3-0.45 Sb_2S_3. Physica Status Solidi (a) 54:67
76. Martens HCF, Blom PWM, Schoo HFM (2000) Comparative study of hole transport in poly(*p*-phenylene vinylene) derivatives. Phys Rev B 61:7489
77. Young RH (1994) Trap-free space-charge-limited current – analytical solution for an arbitrary mobility law. Phil Mag Lett 70:331
78. Abkowitz M, Pai DM (1986) Comparison of the drift mobility measured under transient and steady-state conditions in a prototypical hopping system. Phil Mag B 53:193
79. Young RH (1994) A law of corresponding states for hopping transport in disordered materials. Phil Mag B 69:577
80. Laquai F, Wegner G, Im C, Bässler H, Heun S (2006) Nondispersive hole transport in carbazole- and anthracene-containing polyspirobifluorene copolymers studied by the charge-generation layer time-of-flight technique. J Appl Phys 99:033710
81. Laquai F, Wegner G, Im C, Bässler H, Heun S (2006) Comparative study of hole transport in polyspirobifluorene polymers measured by the charge-generation layer time-of-flight technique. J Appl Phys 99:023712
82. Bao Z, Dodabalapur A, Lovinger AJ (1996) Soluble and processable regioregular poly (3-hexylthiophene) for thin film field-effect transistor applications with high mobility. Appl Phys Lett 69:4108
83. Sirringhaus H, Brown PJ, Friend RH, Nielsen MM, Bechgaard K, Langeveld-Voss BMW, Spiering AJH, Janssen RAJ, Meijer EW, Herwig P, de Leeuw DM (1999) Two-dimensional charge transport in self-organized, high-mobility conjugated polymers. Nature 401:685
84. Brown PJ, Sirringhaus H, Harrison M, Shkunov M, Friend RH (2001) Optical spectroscopy of field-induced charge in self-organized high mobility poly(3-hexylthiophene). Phys Rev B 63:125204
85. Brown PJ, Thomas DS, Köhler A, Wilson JS, Kim J-S, Ramsdale CM, Sirringhaus H, Friend RH (2003) Effect of interchain interactions on the absorption and emission of poly (3-hexylthiophene). Phys Rev B 67:064203
86. Khan RUA, Poplavskyy D, Kreouzis T, Bradley DDC (2007) Hole mobility within arylamine-containing polyfluorene copolymers: a time-of-flight transient-photocurrent study. Phys Rev B 75:035215
87. Kreouzis T, Poplavskyy D, Tuladhar SM, Campoy-Quiles M, Nelson J, Campbell AJ, Bradley DDC (2006) Temperature and field dependence of hole mobility in poly (9,9-dioctylfluorene). Phys Rev B 73:235201
88. Scherf U, List EJW (2002) Semiconducting polyfluorenes – towards reliable structure–-property relationships. Adv Mater 14:477
89. Khan ALT, Sreearunothai P, Herz LM, Banach MJ, Köhler A (2004) Morphology-dependent energy transfer within polyfluorene thin films. Phys Rev B 69:085201
90. Van Mensfoort SLM, Vulto SIE, Janssen RAJ, Coehoorn R (2008) Hole transport in polyfluorene-based sandwich-type devices: quantitative analysis of the role of energetic disorder. Phys Rev B 78:085208
91. Mozer AJ, Sariciftci NS, Pivrikas A, Österbacka R, Juska G, Brassat L, Bässler H (2005) Charge carrier mobility in regioregular poly(3-hexylthiophene) probed by transient conductivity techniques: a comparative study. Phys Rev B 71:035214
92. Meisel KD, Vocks H, Bobbert PA (2005) Polarons in semiconducting polymers: study within an extended Holstein model. Phys Rev B 71:205206
93. Mohan SR, Joshi MP, Singh MP (2009) Negative electric field dependence of mobility in TPD doped polystyrene. Chem Phys Lett 470:279

94. Tanase C, Wildeman J, Blom PWM, Mena Benito ME, de Leeuw DM, van Breemen AJJM, Herwig PT, Chlon CHT, Sweelssen J, Schoo HFM (2005) Optimization of the charge transport in poly(phenylene vinylene) derivatives by processing and chemical modification. J Appl Phys 97:123703
95. Van Mensfoort SLM, Coehoorn R (2008) Effect of Gaussian disorder on the voltage dependence of the current density in sandwich-type devices based on organic semiconductors. Phys Rev B 78:085207
96. Pasveer WF, Cottaar J, Tanase C, Coehoorn R, Bobbert PA, Blom PWM, de Leeuw DM, Michels MAJ (2005) Unified description of charge-carrier mobilities in disordered semiconducting polymers. Phys Rev Lett 94:206601
97. Arkhipov VI, Heremans P, Emelianova EV, Adriaenssens GJ, Bässler H (2002) Weak-field carrier hopping in disordered organic semiconductors: the effects of deep traps and partly filled density-of-states distribution. J Phys Condens Matter 14:9899
98. Coehoorn R, Pasveer WF, Bobbert PA, Michels MAJ (2005) Charge-carrier concentration dependence of the hopping mobility in organic materials with Gaussian disorder. Phys Rev B 72:155206
99. Coehoorn R (2007) Hopping mobility of charge carriers in disordered organic host-guest systems: dependence on the charge-carrier concentration. Phys Rev B 75:155203
100. Fishchuk II, Arkhipov VI, Kadashchuk A, Heremans P, Bässler H (2007) Analytic model of hopping mobility at large charge carrier concentrations in disordered organic semiconductors: polarons versus bare charge carriers. Phys Rev B 76:045210
101. Arkhipov VI, Emelianova EV, Heremans P, Bässler H (2005) Analytic model of carrier mobility in doped disordered organic semiconductors. Phys Rev B 72:235202
102. Fishchuk II, Kadashchuk AK, Genoe J, Ullah M, Sitter H, Singh TB, Sariciftci NS, Bässler H (2010) Temperature dependence of the charge carrier mobility in disordered organic semiconductors at large carrier concentrations. Phys Rev B 81:045202
103. Emin D (2008) Generalized adiabatic polaron hopping: Meyer-Neldel compensation and Poole-Frenkel behavior. Phys Rev Lett 100:166602
104. Craciun NI, Wildeman J, Blom PWM (2008) Universal Arrhenius temperature activated charge transport in diodes from disordered organic semiconductors. Phys Rev Lett 100:056601
105. Blakesley JC, Clubb HS, Greenham NC (2010) Temperature-dependent electron and hole transport in disordered semiconducting polymers: analysis of energetic disorder. Phys Rev B 81:045210
106. Agrawal R, Kumar P, Ghosh S, Mahapatro AK (2008) Thickness dependence of space charge limited current and injection limited current in organic molecular semiconductors. Appl Phys Lett 93:073311
107. Walzer K, Maennig B, Pfeiffer M, Leo K (2007) Highly efficient organic devices based on electrically doped transport layers. Chem Rev 107:1233
108. Chiang CK, Fincher CR, Park JYW, Heeger AJ, Shirakawa H, Louis EJ, Gau SC, MacDiarmid AG (1977) Electrical conductivity in doped polyacetylene. Phys Rev Lett 39:1098
109. Heeger AJ (1989) Charge transfer in conducting polymers. Striving toward intrinsic properties. Faraday Discuss Chem Soc 88:203
110. Pfeiffer M, Fritz T, Blochwitz J, Nollau A, Plönnigs B, Beyer A, Leo K (1999) Controlled doping of molecular organic layers: physics and device prospects. Adv Sol State Phys 39:77
111. Gao W, Kahn A (2001) Controlled p-doping of zinc phthalocyanine by coevaporation with tetrafluorotetracyanoquinodimethane: a direct and inverse photoemission study. Appl Phys Lett 79:4040
112. Matsushima T, Adachi C (2008) Enhancing hole transports and generating hole traps by doping organic hole-transport layers with p-type molecules of 2,3,5,6-tetrafluoro-7,7,8,8-tetracyanoquinodimethane. Thin Solid Films 517:874

113. Lee J-H, Leem D-S, Kim J-J (2010) Effect of host organic semiconductors on electrical doping. Org Electron 11:486
114. Zhang Y, de Boer B, Blom PWM (2009) Controllable molecular doping and charge transport in solution-processed polymer semiconducting layers. Adv Funct Mater 19:1901
115. Maennig B, Pfeiffer M, Nollau A, Zhou X, Leo K, Simon P (2001) Controlled p-type doping of polycrystalline and amorphous organic layers: self-consistent description of conductivity and field-effect mobility by a microscopic percolation model. Phys Rev B 64:195208
116. Kido J, Nagai K, Okamoto Y (1993) Bright organic electroluminescent devices with double-layer cathode. IEEE Trans Electron Devices 40:1342
117. Nollau A, Pfeiffer M, Fritz T, Leo K (2000) Controlled n-type doping of a molecular organic semiconductor: naphthalenetetracarboxylic dianhydride (NTCDA) doped with bis (ethylenedithio)-tetrathiafulvalene (BEDT-TTF). J Appl Phys 87:4340
118. Tanaka S, Kanai K, Kawabe E, Iwahashi T, Nishi T, Ouchi Y, Seki K (2005) Doping effect of tetrathianaphthacene molecule in organic semiconductors on their interfacial electronic structures studied by UV photoemission spectroscopy. Jpn J Appl Phys 44:3760
119. Chan CK, Amy F, Zhang Q, Barlow S, Marder S, Kahn A (2006) N-Type doping of an electron-transport material by controlled gas-phase incorporation of cobaltocene. Chem Phys Lett 431:67
120. Werner AG, Li F, Harada K, Pfeiffer M, Fritz T, Leo K (2003) Pyronin B as a donor for n-type doping of organic thin films. Appl Phys Lett 82:4495
121. Werner A, Li F, Harada K, Pfeiffer M, Fritz T, Leo K, Machill S (2004) n-Type doping of organic thin films using cationic dyes. Adv Funct Mater 14:255
122. Hulea IN, Brom HB, Houtepen AJ, Vanmaekelbergh D, Kelly JJ, Meulenkamp EA (2004) Wide energy-window view on the density of states and hole mobility in poly(p-phenylene vinylene). Phys Rev Lett 93:166601
123. Tanase C, Meijer EJ, Blom PWM, de Leeuw DM (2003) Unification of the hole transport in polymeric field-effect transistors and light-emitting diodes. Phys Rev Lett 91:216601
124. Silver M, Pautmeier L, Bässler H (1989) On the origin of exponential band tails in amorphous-semiconductors. Solid State Commun 72:177
125. Arkhipov VI, Heremans P, Emelianova EV, Bässler H (2005) Effect of doping on the density-of-states distribution and carrier hopping in disordered organic semiconductors. Phys Rev B 71:045214
126. Zhou J, Zhou YC, Zhao JM, Wu CQ, Ding XM, Hou XY (2007) Carrier density dependence of mobility in organic solids: a Monte Carlo simulation. Phys Rev B 75:153201
127. Van der Holst JJM, van Oost FWA, Coehoorn R, Bobbert PA (2009) Electron-hole recombination in disordered organic semiconductors: validity of the Langevin formula. Phys Rev B 80:235202
128. Prigodin VN, Hsu FC, Park JH, Waldmann O, Epstein AJ (2008) Electron-ion interaction in doped conducting polymers. Phys Rev B 78:035203
129. Lee HJ, Lee J, Park S-M (2010) Electrochemistry of conductive polymers. 45. Nanoscale conductivity of PEDOT and PEDOT:PSS composite films studied by current-sensing AFM. J Phys Chem B 114:2660
130. Jung JW, Lee JU, Jo WH (2009) High-efficiency polymer solar cells with water-soluble and self-doped conducting polyaniline graft copolymer as hole transport layer. J Phys Chem C 114:633
131. Banerjee S, Kumar A (2010) Dielectric behavior and charge transport in polyaniline nanofiber reinforced PMMA composites. J Phys Chem Solids 71:381
132. Li D, Huang J, Kaner RB (2009) Polyaniline nanofibers: a unique polymer nanostructure for versatile applications. Acc Chem Res 42:135
133. Lee K, Miller EK, Aleshin AN, Menon R, Heeger AJ, Kim JH, Yoon CO, Lee H (1998) Nature of the metallic state in conducting polypyrrole. Adv Mater 10:456
134. Hulea IN, Brom HB, Mukherjee AK, Menon R (2005) Doping, density of states, and conductivity in polypyrrole and poly(p-phenylene vinylene). Phys Rev B 72:054208

135. Mott NF (1969) Conduction in non-crystalline materials. 3. Localized states in a pseudogap and near extremities of conduction and valence bands. Phil Mag 19:835
136. Weiser G, Möller S (2002) Directional dispersion of the optical resonance of π-π* transitions of alpha-sexithiophene single crystals. Phys Rev B 65:045203
137. Zuilhof H, Barentsen HM, van Dijk M, Sudhölter EJR, Hoofman RJOM, Siebbeles LDA, de Haas MP, Warman JM (2001) In: Nalwa HS (ed) Supramolecular photosensitive and electroactive materials. Elsevier, San Diego
138. Milota F, Sperling J, Szöcs V, Tortschanoff A, Kauffmann HF (2004) Correlation of femtosecond wave packets and fluorescence interference in a conjugated polymer: towards the measurement of site homogeneous dephasing. J Chem Phys 120:9870
139. Dykstra TE, Kovalevskij V, Yang X, Scholes GD (2005) Excited state dynamics of a conformationally disordered conjugated polymer: a comparison of solutions and film. Chem Phys 318:21
140. Gelinck GH, Warman JM (1996) Charge carrier dynamics in pulse-irradiated polyphenylenevinylenes: effects of broken conjugation, temperature, and accumulated dose. J Phys Chem 100:20035
141. Prins P, Candeias LP, van Breemen AJJM, Sweelssen J, Herwig PT, Schoo HFM, Siebbeles LDA (2005) Electron and hole dynamics on isolated chains of a solution-processable poly (thienylenevinylene) derivative in dilute solution. Adv Mater 17:718
142. Huitema HEA, Gelinck GH, van der Putten JBPH, Kuijk KE, Hart CM, Cantatore E, de Leeuw DM (2002) Active-matrix displays driven by solution-processed polymeric transistors. Adv Mater 14:1201
143. Grozema FC, van Duijnen PT, Berlin YA, Ratner MA, Siebbeles LDA (2002) Intramolecular charge transport along isolated chains of conjugated polymers: effect of torsional disorder and polymerization defects. J Phys Chem B 106:7791
144. Warman JM, de Haas MP, Dicker G, Grozema FC, Piris J, Debije MG (2004) Charge mobilities in organic semiconducting materials determined by pulse-radiolysis time-resolved microwave conductivity: π-bond-conjugated polymers versus π−π-stacked discotics. Chem Mater 16:4600
145. Adam D, Schuhmacher P, Simmerer J, Häussling L, Siemensmeyer K, Etzbach KH, Ringsdorf H, Haarer D (1994) Fast photoconduction in the highly ordered columnar phase of a discotic liquid-crystal. Nature 371:141
146. Pingel P, Zen A, Abellon RD, Grozema FC, Siebbeles LDA, Neher D (2010) Temperature-resolved local and macroscopic charge carrier transport in thin P3HT layers. Adv Funct Mater 20:2286
147. Joshi S, Grigorian S, Pietsch U, Pingel P, Zen A, Neher D, Scherf U (2008) Thickness dependence of the crystalline structure and hole mobility in thin films of low molecular weight poly(3-hexylthiophene). Macromolecules 41:6800
148. Prins P, Grozema FC, Siebbeles LDA (2006) Efficient charge transport along phenylene-vinylene molecular wires. J Phys Chem B 110:14659
149. Prins P, Grozema FC, Schins JM, Savenije TJ, Patil S, Scherf U, Siebbeles LDA (2006) Effect of intermolecular disorder on the intrachain charge transport in ladder-type poly (p-phenylenes). Phys Rev B 73:045204
150. Prins P, Grozema FC, Schins JM, Patil S, Scherf U, Siebbeles LDA (2006) High intrachain hole mobility on molecular wires of ladder-type poly(*p*-phenylenes). Phys Rev Lett 96:146601
151. Parkinson P, Joyce HJ, Gao Q, Tan HH, Zhang X, Zou J, Jagadish C, Herz LM, Johnston MB (2009) Carrier lifetime and mobility enhancement in nearly defect-free core-shell nanowires measured using time-resolved terahertz spectroscopy. Nano Lett 9:3349
152. Parkinson P, Lloyd-Hughes J, Johnston MB, Herz LM (2008) Efficient generation of charges via below-gap photoexcitation of polymer-fullerene blend films investigated by terahertz spectroscopy. Phys Rev B 78:115321

153. Němec H, Nienhuys H-K, Perzon E, Zhang F, Inganäs O, Kužel P, Sundström V (2009) Ultrafast conductivity in a low-band-gap polyphenylene and fullerene blend studied by terahertz spectroscopy. Phys Rev B 79:245326
154. Devižis A, Serbenta A, Meerholz K, Hertel D, Gulbinas V (2009) Ultrafast dynamics of carrier mobility in a conjugated polymer probed at molecular and microscopic length scales. Phys Rev Lett 103:027404
155. Warta W, Karl N (1985) Hot holes in naphthalene: high, electric-field-dependent mobilities. Phys Rev B 32:1172
156. Silinsh EA, Capek V (1994) Organic molecular crystals. Interaction, localization and transport properties. American Institute of Physics, New York
157. Fratini S, Ciuchi S (2009) Bandlike motion and mobility saturation in organic molecular semiconductors. Phys Rev Lett 103:266601
158. Hasegawa T, Takeya J (2009) Organic field-effect transistors using single crystals. Science Tech Adv Mater 10:024314
159. Podzorov V, Menard E, Borissov A, Kiryukhin V, Rogers JA, Gershenson ME (2004) Intrinsic charge transport on the surface of organic semiconductors. Phys Rev Lett 93:086602
160. Zeis R, Besnard C, Siegrist T, Schlockermann C, Chi X, Kloc C (2006) Field effect studies on rubrene and impurities of rubrene. Chem Mater 18:244
161. Wang L, Fine D, Basu D, Dodabalapur A (2007) Electric-field-dependent charge transport in organic thin-film transistors. J Appl Phys 101:054515
162. Jurchescu OD, Baas J, Palstra TTM (2004) Effect of impurities on the mobility of single crystal pentacene. Appl Phys Lett 84:3061
163. Koch N, Vollmer A, Salzmann I, Nickel B, Weiss H, Rabe JP (2006) Evidence for temperature-dependent electron band dispersion in pentacene. Phys Rev Lett 96:156803
164. Minari T, Nemoto T, Isoda S (2006) Temperature and electric-field dependence of the mobility of a single-grain pentacene field-effect transistor. J Appl Phys 99:034506
165. Hamadani BH, Richter CA, Gundlach DJ, Kline RJ, McCulloch I, Heeney M (2007) Influence of source-drain electric field on mobility and charge transport in organic field-effect transistors. J Appl Phys 102:044503
166. Hallam T, Lee M, Zhao N, Nandhakumar I, Kemerink M, Heeney M, McCulloch I, Sirringhaus H (2009) Local charge trapping in conjugated polymers resolved by scanning Kelvin probe microscopy. Phys Rev Lett 103:256803
167. Sakanoue T, Sirringhaus H (2010) Band-like temperature dependence of mobility in a solution-processed organic semiconductor. Nat Mater 9:736
168. Yuen JD, Menon R, Coates NE, Namdas EB, Cho S, Hannahs ST, Moses D, Heeger AJ (2009) Nonlinear transport in semiconducting polymers at high carrier densities. Nat Mater 8:572
169. Wolf U, Arkhipov VI, Bässler H (1999) Current injection from a metal to a disordered hopping system. I. Monte Carlo simulation. Phys Rev B 59:7507
170. Arkhipov VI, Wolf U, Bässler H (1999) Current injection from a metal to a disordered hopping system. II. Comparison between analytic theory and simulation. Phys Rev B 59:7514
171. Gartstein YN, Conwell EM (1995) High-field hopping mobility in molecular systems with spatially correlated energetic disorder. Chem Phys Lett 245:351
172. Akuetey G, Hirsch J (1991) Contact-injected currents in polyvinylcarbazole. Phil Mag B 63:389
173. Van Woudenbergh T, Blom PWM, Vissenberg MCJM, Huiberts JN (2001) Temperature dependence of the charge injection in poly-dialkoxy-*p*-phenylene vinylene. Appl Phys Lett 79:1697
174. Hosseini AR, Wong MH, Shen Y, Malliaras GG (2005) Charge injection in doped organic semiconductors. J Appl Phys 97:023705
175. Burin AL, Ratner MA (2000) Temperature and field dependence of the charge injection from metal electrodes into random organic media. J Chem Phys 113:3941

176. Ishii H, Sugiyama K, Ito E, Seki K (1999) Energy level alignment and interfacial electronic structures at organic/metal and organic/organic interfaces. Adv Mater 11:605
177. Koch N, Elschner A, Johnson RL, Rabe JP (2005) Energy level alignment at interfaces with pentacene: metals versus conducting polymers. Appl Surf Sci 244:593
178. Blakesley JC, Greenham NC (2009) Charge transfer at polymer-electrode interfaces: the effect of energetic disorder and thermal injection on band bending and open-circuit voltage. J Appl Phys 106:034507
179. Steyrleuthner R, Schubert M, Jaiser F, Blakesley JC, Chen Z, Facchetti A, Neher D (2010) Bulk electron transport and charge injection in a high mobility n-type semiconducting polymer. Adv Mater 22:2799
180. Davids PS, Campbell IH, Smith DL (1997) Device model for single carrier organic diodes. J Appl Phys 82:6319
181. Wolf U, Barth S, Bässler H (1999) Electrode versus space-charge-limited conduction in organic light-emitting diodes. Appl Phys Lett 75:2035
182. Koo Y-M, Choi S-J, Chu T-Y, Song O-K, Shin W-J, Lee J-Y, Kim JC, Yoon T-H (2008) Ohmic contact probed by dark injection space-charge-limited current measurements. J Appl Phys 104:123707
183. Wang ZB, Helander MG, Greiner MT, Qiu J, Lu ZH (2009) Energy-level alignment and charge injection at metal/C_{60}/organic interfaces. Appl Phys Lett 95:043302
184. Fehse K, Olthof S, Walzer K, Leo K, Johnson RL, Glowatzki H, Broker B, Koch N (2007) Energy level alignment of electrically doped hole transport layers with transparent and conductive indium tin oxide and polymer anodes. J Appl Phys 102:073719
185. Cheng X, Noh Y-Y, Wang J, Tello M, Frisch J, Blum R-P, Vollmer A, Rabe JP, Koch N, Sirringhaus H (2009) Controlling electron and hole charge injection in ambipolar organic field-effect transistors by self-assembled monolayers. Adv Funct Mater 19:2407
186. Wolf U, Bässler H (1999) Enhanced electron injection into light-emitting diodes via interfacial tunneling. Appl Phys Lett 74:3848
187. Abkowitz M, Facci JS, Stolka M (1993) Time-resolved space charge-limited injection in a trap-free glassy polymer. Chem Phys 177:783
188. Fong HH, Papadimitratos A, Hwang J, Kahn A, Malliaras GG (2009) Hole injection in a model fluorene–triarylamine copolymer. Adv Funct Mater 19:304
189. Arkhipov VI, Heremans P, Bässler H (2003) Why is exciton dissociation so efficient at the interface between a conjugated polymer and an electron acceptor? Appl Phys Lett 82:4605
190. Albrecht U, Bässler H (1995) Yield of geminate pair dissociation in an energetically random hopping system. Chem Phys Lett 235:389
191. Emelianova EV, van der Auweraer M, Bässler H (2008) Hopping approach towards exciton dissociation in conjugated polymers. J Chem Phys 128:224709
192. Rubel O, Baranovskii SD, Stolz W, Gebhard F (2008) Exact solution for hopping dissociation of geminate electron-hole pairs in a disordered chain. Phys Rev Lett 100:196602
193. Deibel C, Strobel T, Dyakonov V (2009) Origin of the efficient polaron-pair dissociation in polymer-fullerene blends. Phys Rev Lett 103:036402
194. Bredas JL, Norton JE, Cornil J, Coropceanu V (2009) Molecular understanding of organic solar cells: the challenges. Acc Chem Res 42:1691
195. Marsh RA, Hodgkiss JM, Friend RH (2010) Direct measurement of electric field-assisted charge separation in polymer: fullerene photovoltaic diodes. Adv Mater 22:3672
196. Hodgkiss JM, Campbell AR, Marsh RA, Rao A, Albert-Seifried S, Friend RH (2010) Subnanosecond geminate charge recombination in polymer-polymer photovoltaic devices. Phys Rev Lett 104:177701
197. Schubert M, Yin CH, Castellani M, Bange S, Tam TL, Sellinger A, Horhold HH, Kietzke T, Neher D (2009) Heterojunction topology versus fill factor correlations in novel hybrid small-molecular/polymeric solar cells. J Chem Phys 130:094703